Report to Professor Paulo Artaxo, University of São Paulo, Brazil and
NASA Goddard Space Flight Center (Purchase Order No. S-97728-Z)

# Scientific Studies During the 1997 Burning Season at Alta Floresta, Brazil

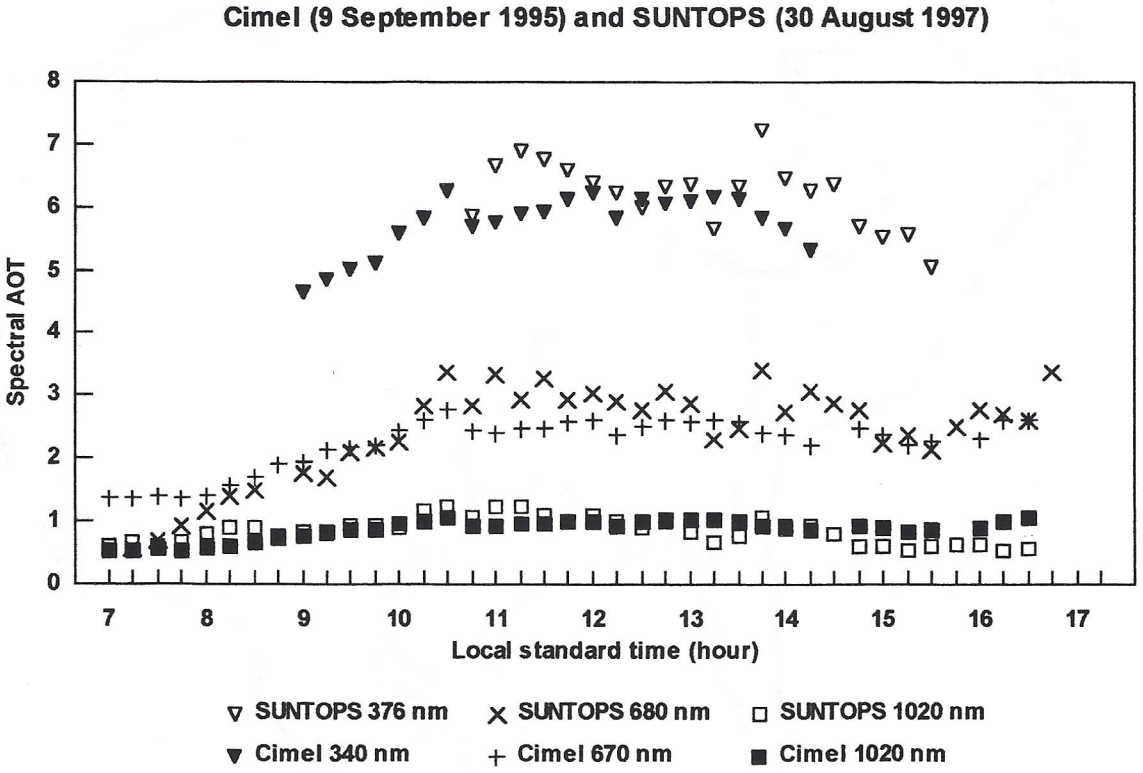



## Forrest M. Mims III

**Sun Photometer Atmospheric Network (SPAN)**
**433 Twin Oak Road, Seguin, Texas 78155 USA**
**fmims@aol.com**

## Bradley S. White

**Texas Lutheran University, Seguin, Texas 78155 USA**


**23 February 1998**

# Contents

Prof. Paulo Artaxo
Instituto de Fisica
Universidade de São Paulo
Caixa Postal 66318
São Paulo, SP
CEP 05389-970
Brazil

P. K. Bhartia
Laboratory for Atmospheres, Code 916
Goddard Space Flight Center
Greenbelt, MD 20771 USA

Brent Holben
Contracting Officer Representative
Laboratory for Terrestrial Physics, Code 923
Goddard Space Flight Center
Greenbelt, MD 20771 USA

Re. Letter of Invitation from Paulo Artaxo and Purchase Order No. S-97728-Z from NASA Goddard Space Flight Center

Dear Drs. Artaxo, Bhartia and Holben:

Enclosed is "Scientific Studies During the 1997 Burning Season at Alta Floresta, Brazil." This report summarizes observations in Brazil conducted at the invitation of Paulo Artaxo and funded through a purchase order from NASA Goddard Space Flight Center suggested by P. K. Bhartia and administered by Brent Holben. I am most grateful for Dr. Artaxo's invitation, the funding provided by NASA GSFC and Brent Holben's comments about the preliminary report. In view of his dedication in assisting with hundreds of optical depth and total ozone observations, I have listed Bradley S. White as a co-author. Mr. White, who is a student at Texas Lutheran University, volunteered for this work and paid his own expenses.

Severe aerosol loading caused by widespread biomass burning obscured the sky during more of our stay at Alta Floresta and the nearby Cristalino River. This report describes the effects of this aerosol loading on optical depth and solar irradiance in the ultraviolet, visible and near-infrared. The report also describes various biological effects associated with severe aerosol loading.

This research was greatly assisted by the people of Alta Floresta, especially the management and staff of the Floresta Amazonica Hotel e Turisom Ltda. and health professionals in Alta Floresta. These and others who assisted with this work are listed in the acknowledgments section.

This report is a work in progress. As with previous studies I have conducted with funding from NASA GSFC, this study will be followed by one or more papers. Therefore, I shall be most interested in receiving criticisms of this report and suggestions for improvements. I am especially interested in collaborating with Dr. Artaxo and NASA GSFC on expanding this study. In particular, I am hopeful that they will consider carefully the implications for human health of diminished UV-B and visible sunlight caused by severe air pollution and the potential use of the TOMS aerosol detection capability as a tool to investigate this topic.

Forrest M. Mims III

## Acknowledgments

This work was conducted at the invitation of Professor Paulo Artaxo of the Instituto de Fisica at the Universidade de São Paulo. I am most grateful for this invitation to again conduct research in Brazil and to share data with Prof. Artaxo. I am also appreciative of helpful discussions about aerosol measurements and tree ring studies with Prof. Artaxo and J. Vanderlei Martins at the Universidade de São Paulo on 9 September 1997. Mr. Martins kindly arranged accommodations in São Paulo and went to considerable trouble to drive us to the university. All data acquired during this study will be provided to the Universidade de São Paulo.

Travel and on-site expenses were provided by a purchase order from NASA's Goddard Space Flight Center suggested by P. K. Bhartia and administered by Brent Holben. I am most appreciative for their continued support of this research. And I am especially grateful for their suggestions and for additional suggestions from and discussions with Tom Eck, Jay Herman and Yoram Kaufman, all of NASA's GSFC, and Bill Grant of NASA Langley.

Bradley White, a student at Texas Lutheran University who accompanied me on this trip at his own expense, made many of the Sun photometer measurements, assisted in various experiments and documented highlights of the trip with photographs and in a journal. The wide variety of observations conducted during this study would not have been possible without Brad's assistance.

Bruce Lighthart provided important suggestions regarding the airborne bacteria study.

Vitoria Da Riva Carvalho of Floresta Amazonica Hotel e Turisom Ltda. provided invaluable assistance during this research and arranged a meeting of physicians and biologists in Alta Floresta. Various employees of Floresta Amazonica Hotel e Turisom Ltda. and local physicians, students and citizens also assisted in this research.

Finally, I am most grateful to Dr. Carlos Alberto Redondo and especially Ms. Gisele Cristina de Castro for providing medical statistics for Alta Floresta. Dr. Redondo arranged for this time consuming work, and Ms. de Castro entered the data into a text program and made plots of the data.

## Disclaimers

Errors: Any errors in this report are the responsibility of the first author. Error notifications, suggestions and criticisms will be gratefully received. This report is preliminary in the sense that the principle findings will be submitted in papers to one or more peer-reviewed journals. Published papers based on this work should be cited in lieu of this report.

Instrument Calibrations: The calibrations of certain instruments may be updated during the preparation of preparing papers describing this work. This may cause quantitative changes to some of the plots displayed herein. Any such changes are expected to be minor.

Commercial Products: The mention by name of commercial products does not necessarily constitute an endorsement.

# Smoke Pall and Fires Observed in GOES-8 Imager

**Date: 27-Aug-1997** **Smoke Coverage: ~ 6.0 million km$^2$**

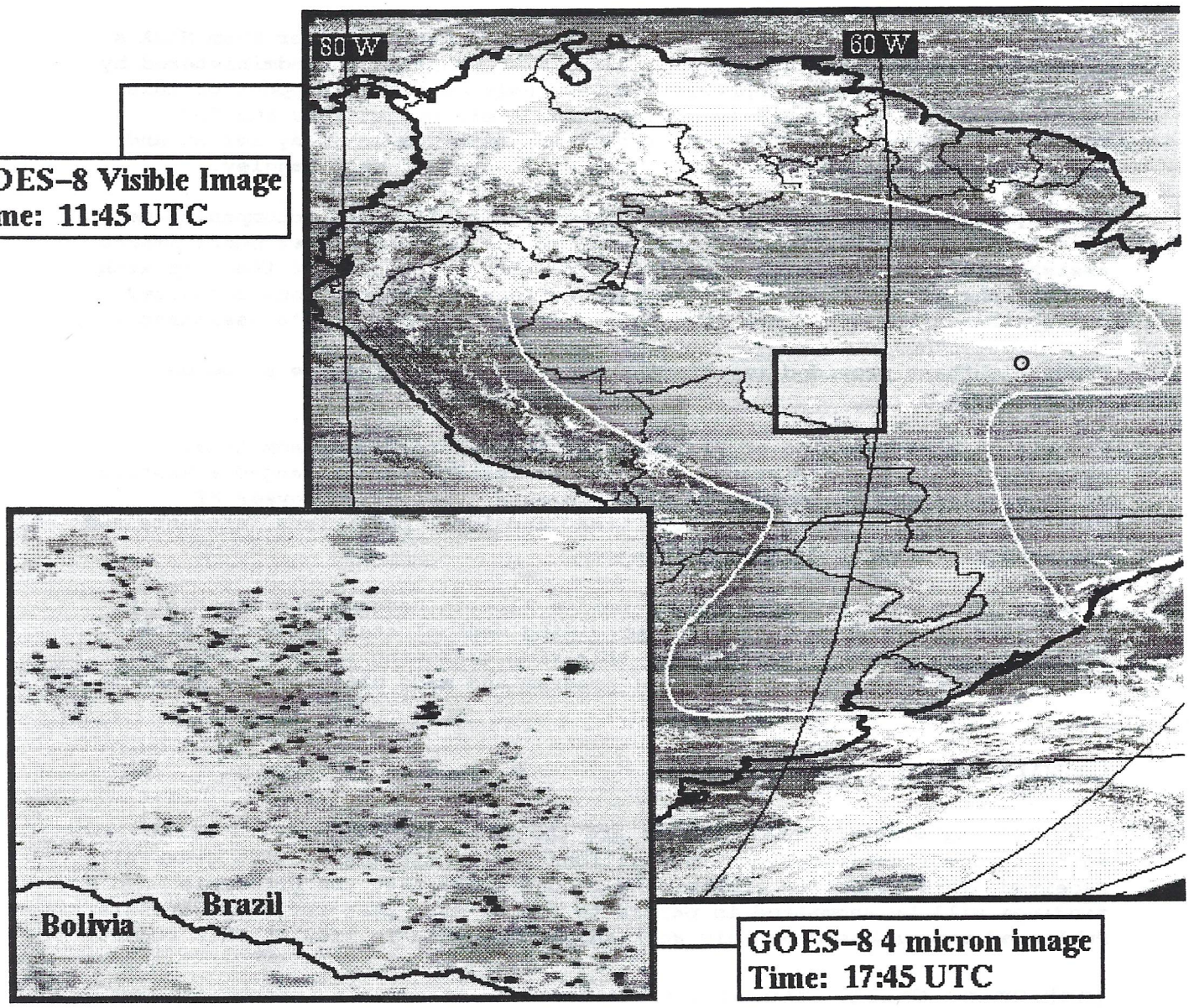

# Abstract

The purpose of this study was to measure various atmospheric and biological effects of severe aerosol loading caused by smoke from biomass burning in and around the remote city of Alta Floresta in west-central Brazil (9.9 S, 55 W) during the 1997 burning season. These studies were among very few conducted during this time in Brazil.

Each day at 15-minute intervals from 22 August to 8 September, measurements were made of the aerosol optical thickness of the atmosphere at various wavelengths and the total column abundance of ozone and water vapor. At solar noon various measurements of diffuse and full-sky irradiance were conducted. Polarization of the zenith sky was measured at sunset. Miniature data loggers recorded temperature and full-sky irradiance at various wavelengths, including UV-B and PAR. On several days measurements of total irradiance at various wavelenghts were conducted under a rain forest canopy and at a nearby open site. Airborne bacteria were collected on sterile agar trays 6 times each day for 8 days. A miniature garden of wheat, corn and beans was raised and the dimensions of principle leaves measured twice each day for 8 days following emergence. A student was hired to compile medical records for 1996-1997.

The principal findings of this work are:

1. The area of smoke coverage over Brazil and adjacent countries on one of the peak burning days in 1997 resembled that on peak burning days in prior years.

2. Significant smoke was present on all days, and on the afternoon of 30 August the optical depth (376 nm) at Alta Floresta exceeded 7.

3. Solar UV-B was reduced below normal levels on all days, and on 30 August the total solar UV-B was reduced to negligible levels. On most days the direct component of the UV-B was reduced to very low levels.

4. The correlation of UV-B at solar noon and ratio of non-pigmented to total airborne bacteria is statistically significant ($r^2 = 0.83$). As most pathogenic bacteria are non-pigmented, this finding may explain some of the increases in respiratory and other diseases that occur during episodes of severe aerosol loading which cause significant reduction in ambient UV-B.

5. The correlations of maximum daily temperature with mean optical depth and total photosynthetic flux are statistically significant ($r^2 = 0.71$ and 0.83, respectively).

6. Photosynthetic flux was reduced below normal levels on most days. A measured consequence of this reduction was leaf elongation in a miniature garden of wheat and corn plants planted at the beginning of this study and observed for 8 days following emergence.

7. Skylight polarization, a navigational cue for various birds, fish and insects, was significantly reduced from normal values on most days.

8. During a seminar for physicians and health professionals in Alta Floresta at which preliminary results of this study were presented, the consensus of those present was that approximately half the population was suffering respiratory illness caused by smoke inhalation.

# 1. INTRODUCTION

In the tropics the maintenance of rangeland and pastures and deforestation for the production of new pastures is generally accompanied by the burning of significant biomass during the dry season. The scale of burning can be so great that prolonged episodes (>60 days) of very severe air pollution can occur. This is the case for large portions of Southeast Asia, Africa and South America, especially in Brazil, Bolivia, Paraguay and Argentina.

The 1988 burning season in Brazil was among the most severe on record. Various press (Lewan, 1997; Beardsley, 1997) and anecdotal reports suggest that the severity of the 1997 burning season may exceed that of 1988, but there is not yet sufficient data to justify this claim. The 1997 burning season occurred during a major ENSO event that caused a significant reduction of rain in much of the Amazon basin. The resultant drying of the tropical forest enhanced the burning phase of deforestation projects and contributed to the spread of intentionally set fires. Of special interest is that many fires occurred deep within the Amazon basin, and smoke caused unprecedented closures of the airport at Manaus and reports of increased respiratory illness. The possibly unprecedented burning near Manaus contributed to speculation about the severity of the 1997 burning season.

Geostationary Operational Environment Satellite (GOES) images of South America on 24 August 1988 show that smoke covered much of Brazil, Bolivia and Paraguay (http://cimss.ssec.wisc.edu/goes/misc/971007.html). A GOES image from 27 August 1997 (Fig. 1) shows that the area of densest smoke coverage closely resembled that on 24 August 1988 (http://cimss.ssec.wisc.edu/goes/burn/ABBAWNDS.GIF).

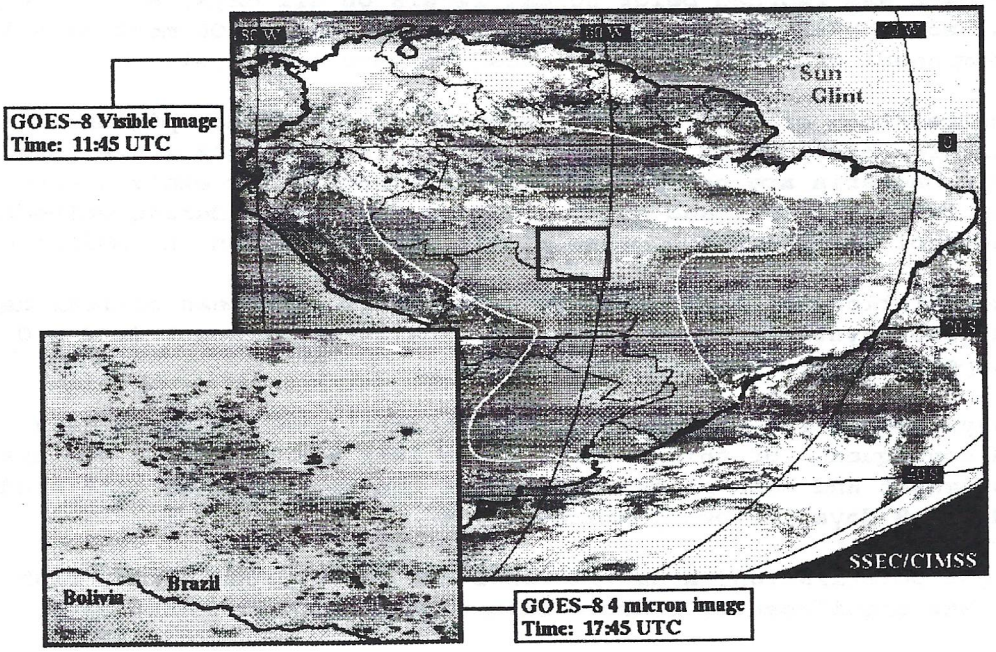


Fig. 1. Smoke observed over South America by GOES-8 on 27 August 1997. Circle denotes Alta Floresta, Brazil (9.9 S, 55 W).

According to an analysis of Fig. 1 by SSEC/CIMSS, smoke covered some 6 million km^2 on 27 August 1997. A preliminary GOES-8 Automated Biomass Burning Algorithm (ABBA) analysis of South America in 1995 yielded from 2,500 to 3,500 fires at 1745 UTC on 12 days during SCAR-B). On 27 August 1997, the GOES-8 ABBA analysis detected 2,695 fires at 1745 UTC (Fig. 2).

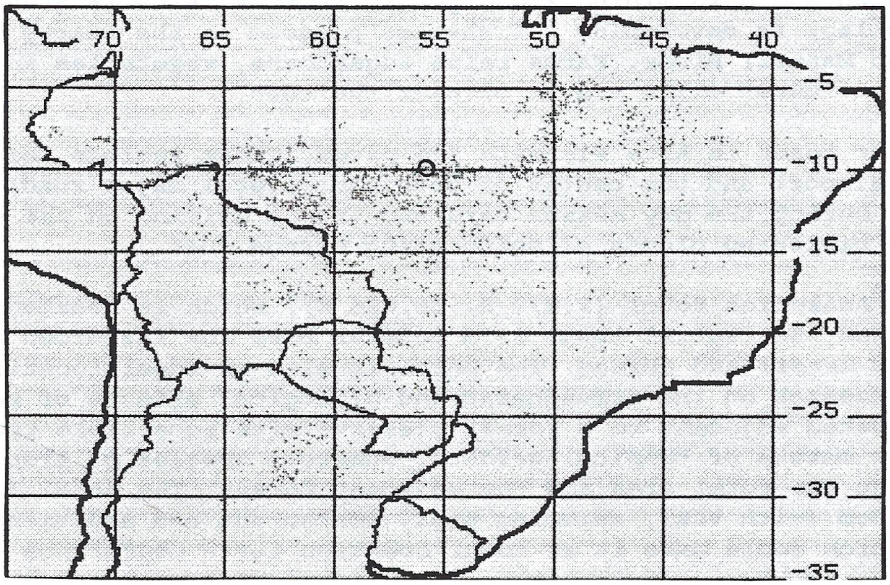


Fig. 2. 2,695 fires detected by ABBA at 1745 UTC on 27 August 1997. Circle denotes Alta Floresta. Courtesy of Elaine Prins *et al.*, Cooperative Institute for Meteorological Satellite Studies (CIMSS), University of Wisconsin-Madison (http://cimss.ssec.wisc.edu/goes/misc/971007.html).

Figure 2 is the only known ABBA fire analysis for the 1997 burning season conducted for South America at the time of this report. The number of fires on this day was at the low end of the most severe burning days in 1995. Thus determining whether or not 1997 was indeed a record burning year must await further ABBA analysis of GOES-8 imagery. Of major interest will be the detection of fires in the Amazon basin itself and especially near Manaus, where thick smoke caused unprecedented airport closures and increased hospitalizations for respiratory problems.

The present study reports only the results of surface measurements. However, various flights over and within Brazil revealed numerous fires (night flights) and considerable smoke. The sky between Cuiabá and Alta Floresta was especially smoky when we flew to Alta Floresta on 21 August and departed on 8 September. Before leaving Cuiaba for São Paulo via Brasilia during SCAR-B on 8 September 1995, the sky over Cuiaba was very smoky ($AOT_{1020\ nm}$ = 0.36 at 1142), but the sky over Brasilia was relatively clear ($AOT_{1020\ nm}$ = 0.07 at 1613 on ramp at Goiana airport). While flying this same route on 8 September 1997, Cuiabá was slightly clearer than on 8 September 1995 ($AOT_{1020\ nm}$ and 0.29 at 1319) but considerable smoke was observed in the sky over Brasilia (AOT not measured).

## 1.1. Alta Floresta

Alta Floresta is a fast-growing frontier town near the remote northern border of Mato Grosso, Brazil. The town is believed to have a population of >70,000. Alta Floresta is accessible by a commercial aircraft from Cuiaba (once per day) and a few other major cities. There is also a daily bus from Cuiaba, about 800 km to the south. Alta Floresta was established ca. 1976, and major deforestation in and all around the town has since occurred. Cattle ranching and gold mining are major activities. Rice is grown, and the local college is developing a fisheries program at the nearby Teles Pires (or São Manuel) River. Farms raise sugar cane, vegetables and fruit trees. Several lumber mills are in or near the town.

Only the major roads in Alta Floresta are paved. These include the road between the airport and the center of town and several major roads in the town itself. During the dry season cars and trucks driving on the unpaved roads create billowing clouds of suffocating orange dust.

The Floresta Amazonica Hotel (9.879 S, 56.096 W), which is located between the airport and the central town, is a popular base for fishermen and bird watchers from Brazil and abroad. The hotel is also an ideal location for conducting research on the atmospheric and biological effects of smoke. The hotel is situated adjacent to a forest preserve with accessible trails and 15,000 square meters of tropical gardens. Numerous species of tropical birds frequent the hotel area and the adjacent forest. The hotel features a conference room (with VCR), swimming pool, restaurant and additional facilities which would make it an ideal location for a conference site.

The forest near the hotel was very dry during our stay. Approximately 2 weeks before our arrival, several hectares of land across the road from the hotel property was cleared and burned for a new housing development. The fire jumped the road and ignited the edge of the hotel's forest preserve. A few hundred square meters were burned before heavy equipment arrived and isolated the burning trees with a firebreak.

## 1.2. Cristalino Jungle Lodge

The ultimate destination for many, perhaps most, of the Floresta Amazonica Hotel patrons is the Cristalino Jungle Lodge. The lodge is located on the remote and pristine Cristalino River in the protected Cristalino Forest Preserve. Access to the lodge requires a 2-hour trip by car or van along unpaved roads. The trip provides an excellent opportunity to observe enormous expanses of deforested land on which cattle are being grazed. Small farms and orchards can also be seen along the roads. We observed smoke from burning operations, and we drove past several large fires. The road ends in a dense forest on the south bank of the Teles Pires River (9.636 S, 55.938 W), where boats transport visitors eastward to the Cristalino River and northward to the lodge (9.596 S, 55.932 W).

The lodge is an excellent location for conducting atmospheric and biological measurements of the kind described here. The lodge is surrounded by a dense forest which is accessible via a network of marked trails. Access to more remote sites, including a rock-capped hill that projects well above the forest (9.58 S, 55.919 W), is available by motor boat or canoe. The hill does not afford a complete $2\pi$ steradian field of view of the sky because of small trees on and around the crest. Numerous species of

tropical birds and butterflies can be seen along the Cristalino River. Tapirs, capybara, foxes, deer and other mammals can also be observed. While comparatively few mosquitoes were present during our stay, sweat bees were occasionally a major nuisance. Bees were especially thick at the very hot crest of the rock-capped hill where we hiked to conduct measurements above the surrounding forest. Hats and protective head nets were absolutely essential.

## 1.2. Instruments and Supplies used in Brazil

### Earth Science Instruments and Supplies

- ☐ Backup watch
- ☐ SW radio (fix antenna)
- ☐ Garmin GPS-38 (plus cable!)
- ☐ Point & shoot cameras (2)
- ☐ 35 mm SLR (fisheye and macro lens)
- ☐ Cable release
- ☐ Mini-tripod
- ☐ Mini-light table
- ☐ Film: Kodacolor
- ☐ Film: Kodachrome
- ☐ Film: b&w
- ☐ Thermometer/RH/DP
- ☐ Glass thermometer
- ☐ Windspeed indicator
- ☐ SUNTOPS
- ☐ MTOPS-7
- ☐ Microtops II (plus cable)
- ☐ Microtops II (SUNTOPS)
- ☐ HP-100 (plus cables!)
- ☐ Sarah radiometer
- ☐ Sun probes
- ☐ Shadow disk and spare pennies
- ☐ Polarizer probes
- ☐ Temperature data logger (plus cable)
- ☐ Data loggers for Sun probes
- ☐ Power adaptors for Brazil
- ☐ Sun shade cloth
- ☐ Batteries
- ☐ Tool kit
- ☐ Multimeter
- ☐ Post-It notes
- ☐ Ruler
- ☐ Notebook
- ☐ Paper
- ☐ Connectors/cables for ALL instruments
- ☐ Tool kit
- ☐ Soldering iron
- ☐ Omnibook PC and power supplies
- ☐ Spare mouse
- ☐ Timer
- ☐ Binoculars
- ☐ Inclinometer
- ☐ Protractor
- ☐ Caliper
- ☐ Velcro & rubber bands
- ☐ Bicycle cable to lock all bags together

### Life Science Supplies

- ☐ UV blocking and transmitting film
- ☐ Color filters
- ☐ Polarizer filters
- ☐ Petri plates/covers (d)
- ☐ Blower/impinger
- ☐ Sterile sandwich bags (d)
- ☐ Clear tape (d)
- ☐ Microscope (optional)
- ☐ Sand paper (d)
- ☐ Fresnel lens
- ☐ Agar sterile contact slides (d)
- ☐ HS pathogen water test (d)
- ☐ Plastic squeezers
- ☐ UV light
- ☐ Insect/larvae nets
- ☐ Marking pen
- ☐ Alcohol pads (d)
- ☐ Tree corer & beeswax
- ☐ Cloth gloves (d)
- ☐ Colored cloth squares (insect study)
- ☐ String
- ☐ Aluminum Screen (d)
- ☐ Plastic trays (d)
- ☐ Collecting nets (insect and larvae)
- ☐ VRUs (d)
- ☐ VRU medium (d)

(d denotes disposable supplies)

## 1.4. Daily Measurement Protocol

**The daily measurement protocol generally followed this schedule unless clouds obscured the Sun:**

**0700: Start Sun photometer observations (3 instruments) and continue at 15-minute intervals on the quarter hour for duration of the day.**

**0720-1730: Measure height of all plants in miniature garden (1 of 2 times).**

**0730-0800: First airborne bacteria tray (including UV-B and wind measurements).**

**0900-1000: Count bacteria colonies from 2 days earlier and record results.**

**1005-1100: Photograph agar trays from 2 days earlier.**

**1000-1030: Second airborne bacteria tray (plus UV-B and wind measurements).**

**1150-1210: Measure solar noon diffuse and full sky irradiance.**

**1215-1220: Measure temperature, relative humidity, dew point and pressure.**

**1215-1245: Third airborne bacteria tray (plus UV-B and wind measurements).**

**1430-1500: Fourth airborne bacteria tray (plus UV-B and wind measurements).**

**1710-1740: Fifth airborne bacteria tray (plus UV-B and wind measurements).**

**1710-1735: Horizon observations and photographs from nearby open site.**

**1730-1740: Measure polarization of zenith sky.**

**1745-1800: Measure height of all plants in miniature garden (2 of 2 times).**

**1830-1900: Download all data loggers. Restart temperature logger immediately.**

**2200-2300: Restart full sky irradiance data loggers and replace on roof.**

**2230-2400: Final airborne bacteria tray (plus wind measurements).**

**2400: Determine if planets and/or stars are visible through smoke.**

**As many of these measurements were overlapping, this protocol was possible only by employing two observers. There was little time for breakfast, no time for lunch, but ample time each evening for a substantial meal. Preliminary data analysis, notebook entries, instrument maintenance, sky photographs and other tasks were performed between measurements.**

**As noted above, the protocol was altered when clouds were present at the Sun. It is especially important to avoid making Sun photometer measurements when clouds or cloud fragments obscure part or all of the Sun. However, the very severe aerosol loading at Alta Floresta often made the visual detection of clouds difficult or impossible. Fortunately the presence of clouds at the Sun can be detected as negative spikes in daily plots of the full-sky irradiance data from the data loggers.**

# 2. ATMOSPHERIC MEASUREMENTS

The sky was quite smoky in and near Alta Floresta from 21 August to 8 September. While flying from Cuiaba to Alta Floresta on 21 August and from Alta Floresta to Cuiaba on 8 September, the ground was usually not visible through the smoke unless orange sunglasses were used. Even then it was often difficult to see through the very thick smoke. Cuiaba's sky was very smoky on 8 September. During SCAR-B, a major study of smoke in Brazil during the 1995 burning season, smoke did not extend to Brasilia. On 8 September during the present burning season, smoke extended from Cuiaba to Brasilia and beyond, but the density of the smoke at Brasilia appeared less than that at Cuiaba. Goes satellite imagery confirmed that smoke covered much of Brazil, Bolivia and Paraguay on 27 August

Each day in Alta Floresta more than 18,000 measurements of temperature, water vapor, various wavelengths of sunlight were made using automated radiometers and hand-held Sun photometers. The principal finding of these measurements is that substantial biomass burning continues to occur in and around Alta Floresta. On 30 August, the optical depth of the smoke was so high (>7 at 376 nm) that the Sun could be viewed without sunglasses and a low flying plane attempting to find the airport could be dimly seen for only a second or so as it passed overhead. On this day the solar UV-B was 0 when measured at the usual scale using a calibrated Solar Light Co. detector.

On most days the optical depth at 376 nm reached or exceeded 3. The morning of 28 August was especially unusual as the sky was clear and blue. This provided an excellent opportunity to obtain clear-sky data to compare with the more usual smoky days.

## 2.1. Aerosol Optical Thickness (AOT)

Three Sun photometers (two Microtops II and a Suntops) measured the aerosol optical thickness of the atmosphere every 15 minutes from 07:00 to about 17:00 each day. The wavelengths measured are 297, 305, 310, 340, 376, 380, 440, 540, 850, 860, 900, 940 and 1020 nm. Redundant wavelengths were included in the event of instrument failure.

### 2.1.1. AOT Measurement Methodology

The accuracy of AOT measurements are critically dependent on instrument stability and calibration. The SUNTOPS and one of the Microtops II instruments were calibrated using the Langley method at Mauna Loa Observatory (MLO) in May 1997. The linearity of the least squares regression line of a Langley method calibration is an important indicator of the reliability of the calibration. Figure 3 shows the excellent linearity obtained for the SUNTOPS channels whose data are discussed next. This instrument has little drift, since light-emitting diodes are used as spectrally selective detectors. For example, the extraterrestrial constants (air mass = 0) for the 376 nm channel measured at MLO in 1996 and 1997 agree within 0.4%.

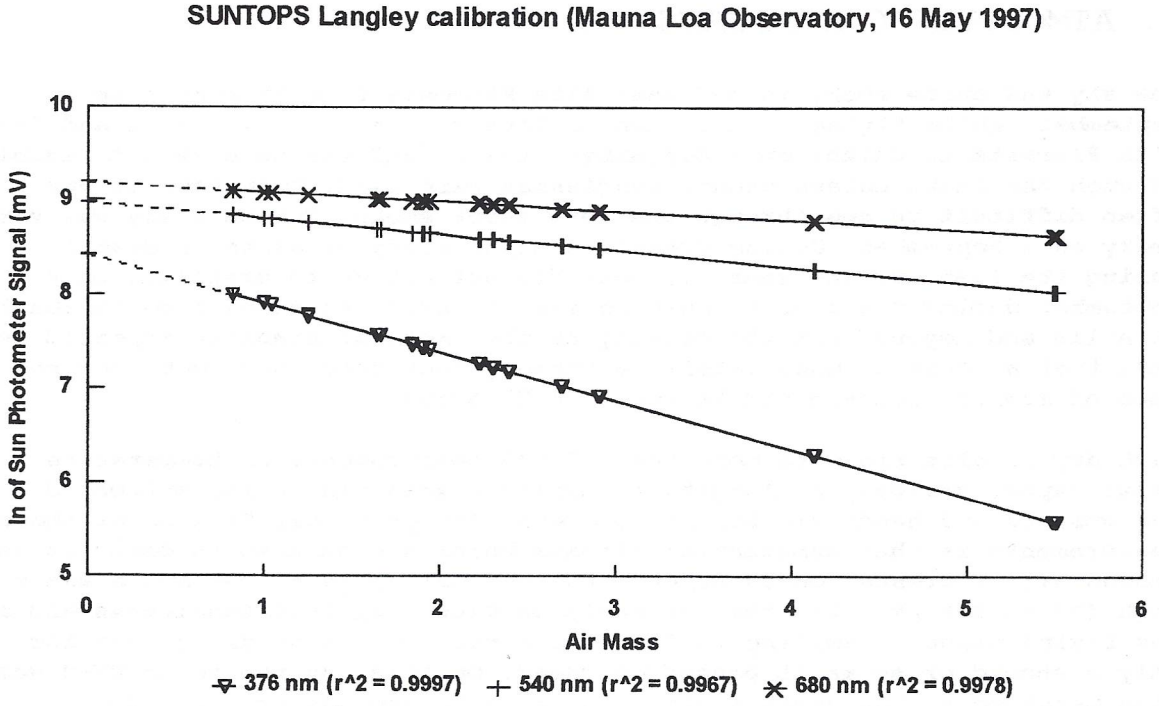


Fig. 3. Langley method calibration of the SUNTOPS Sun Photometer used at Alta Floresta and the Cristalino River site. (Measurements at air mass <1 result from the high altitude of the site, 3.4 km MSL.)

One way to assess the accuracy of SUNTOPS AOT observations is to compare the instrument with a Cimel Sun photometer at the same location. Although a Cimel was not present at Alta Floresta in 1997, one was there in 1995. Figure 4, a comparison of the AOT measured by a Cimel and SUNTOPS on the days with the most severe aerosol loading, shows excellent agreement between these instruments in the presence of very high optical depth. The Cimel data are from Brent Holben at the NASA GSFC Aeronet web site (http://spamer.gsfc.nasa.gov/).

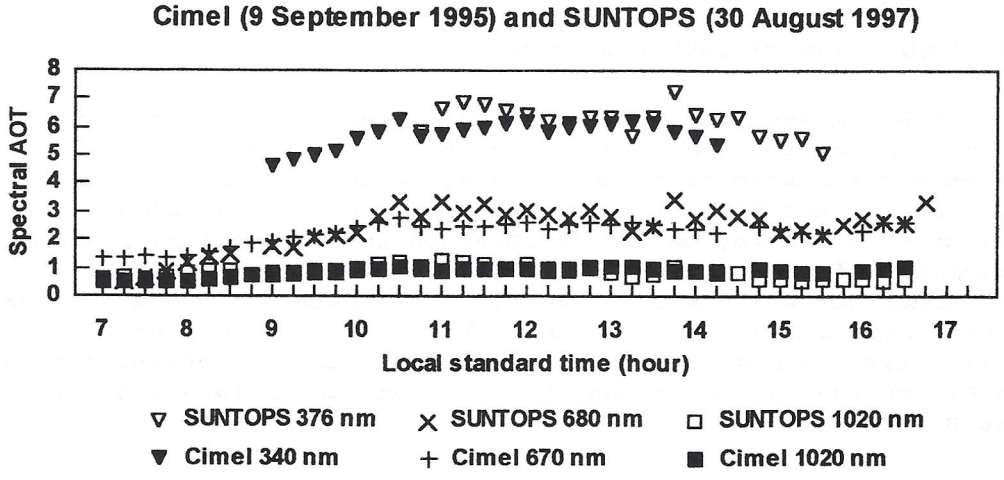


Fig. 4. Comparison of Cimel and SUNTOPS AOT observations at Alta Floresta.

## 2.1.2. AOT Measurement Results

The extremes of AOT occurred on 28 and 30 August (see Figs. 5 and 6). The morning of 28 August was clear, the sky was blue, and optical depths resembled those in a non-polluted region. Extraordinary levels of smoke were present during most of 30 August, and the optical depth at 376 nm exceeded 6 at solar noon. On both days the least AOT occurred in the early morning.

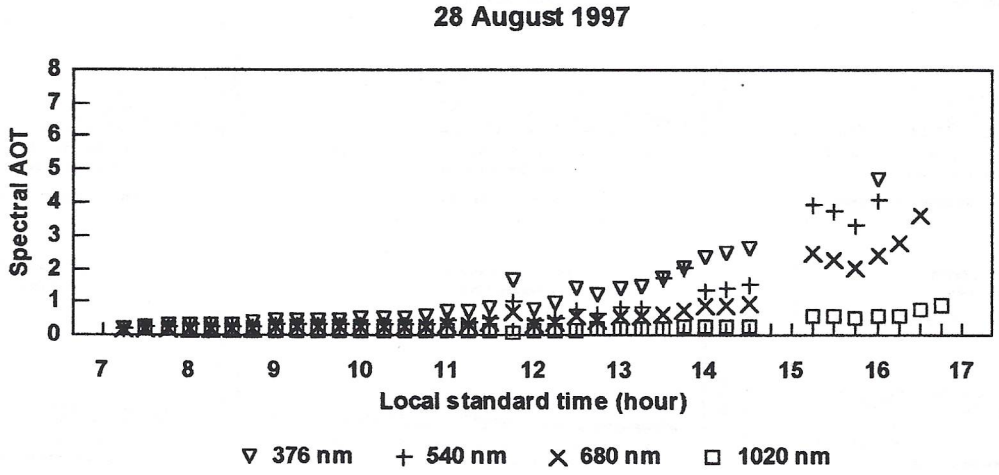


Fig. 5. AOT on the clearest day at Alta Floresta (SUNTOPS). The early morning values resemble those measured in a region with little air pollution.

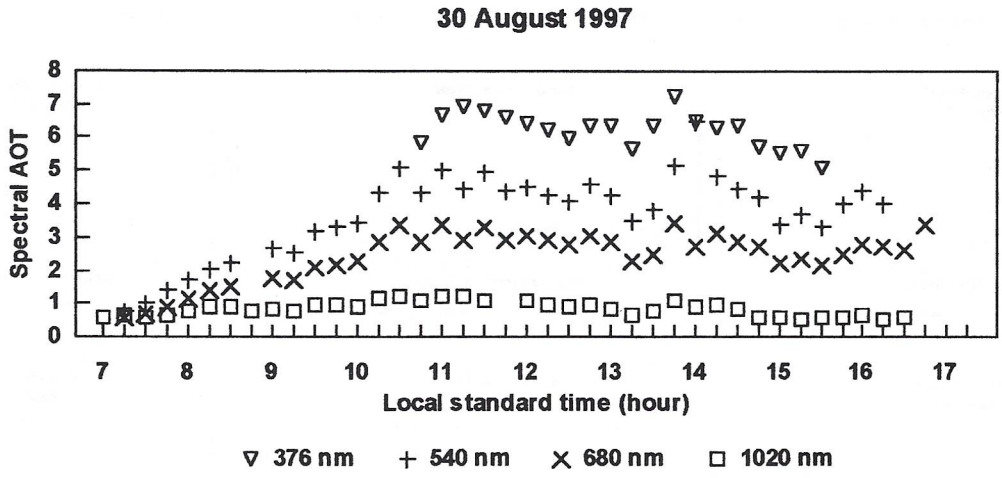


Fig. 6. AOT on the smokiest day at Alta Floresta (SUNTOPS). There is a very rapid increase in AOT in the early morning followed by a sustained very high AOT thereafter.

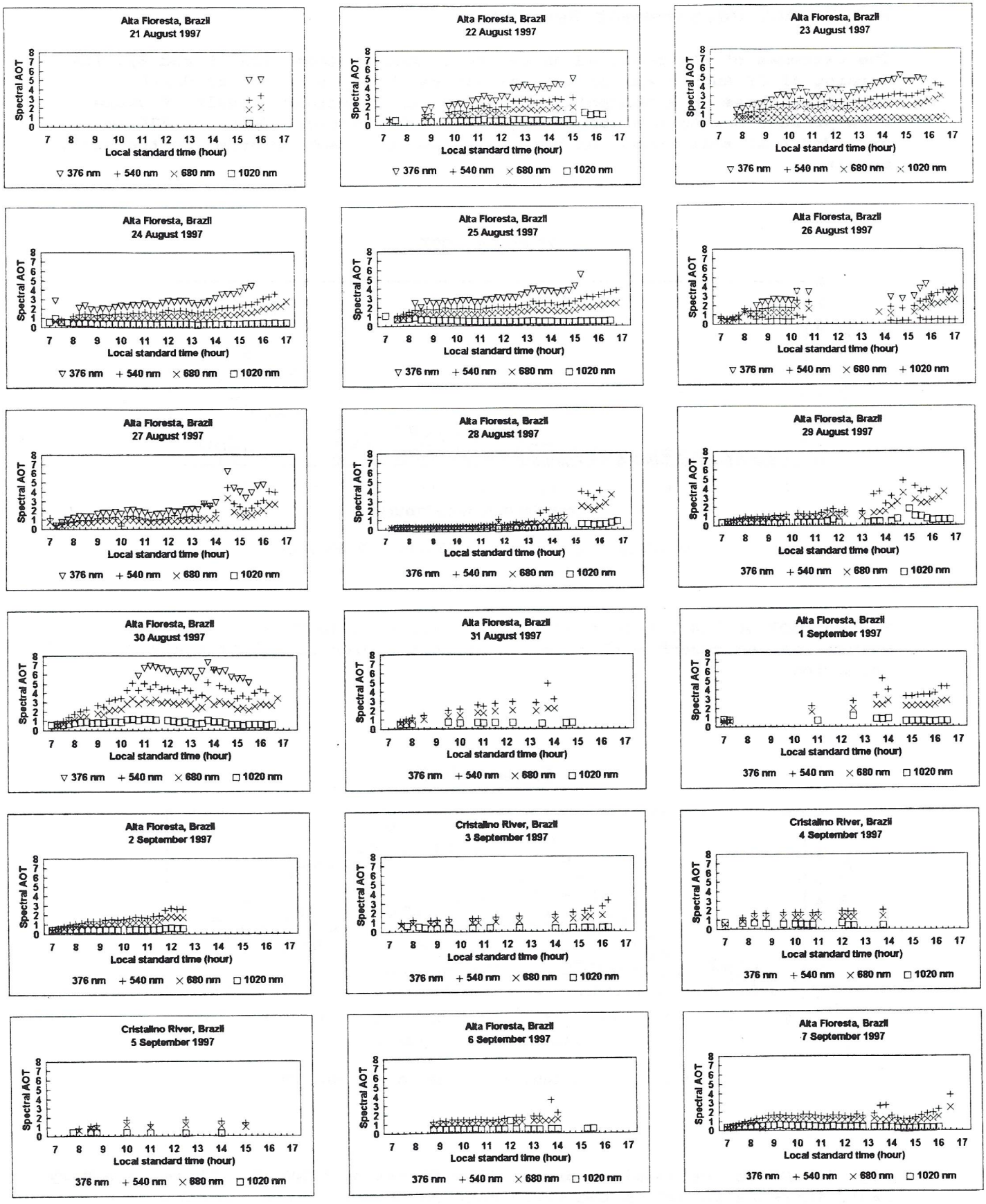


**Fig. 7. Aerosol optical thickness observed by SUNTOPS sun photometer at 15-minute intervals at Alta Floresta and the Cristalino River site.**

## 2.2. Total and Diffuse Solar Irradiance (UV-B, visible and near IR)

Total and diffuse solar irradiance was measured by two digital radiometers with removable probes and 8 data logging radiometers with removable probes. The light-sensitive probes incorporated spectrally selective photodiodes or photodiodes and interference filters. The light probes were equipped with Teflon diffusers to provide a cosine response. Diffuse irradiance was measured by shadowing the Teflon diffuser with a small disk at or near solar noon. Data loggers were programmed to sample the solar irradiance at 24 second intervals for a 12 hour period beginning at 05:50 each morning. The digital radiometers were used at solar noon and during the collection of airborne bacteria.

The most interesting results from this work include the measurement of significantly reduced UV-B and photosynthetic radiation (PAR) during episodes of severe aerosol loading (e.g. 30 August). PAR measurements are discussed in Section 3.2. Figure 8 shows the UV-B index measured at 24-second intervals on the clearest and smokiest days at Alta Floresta.

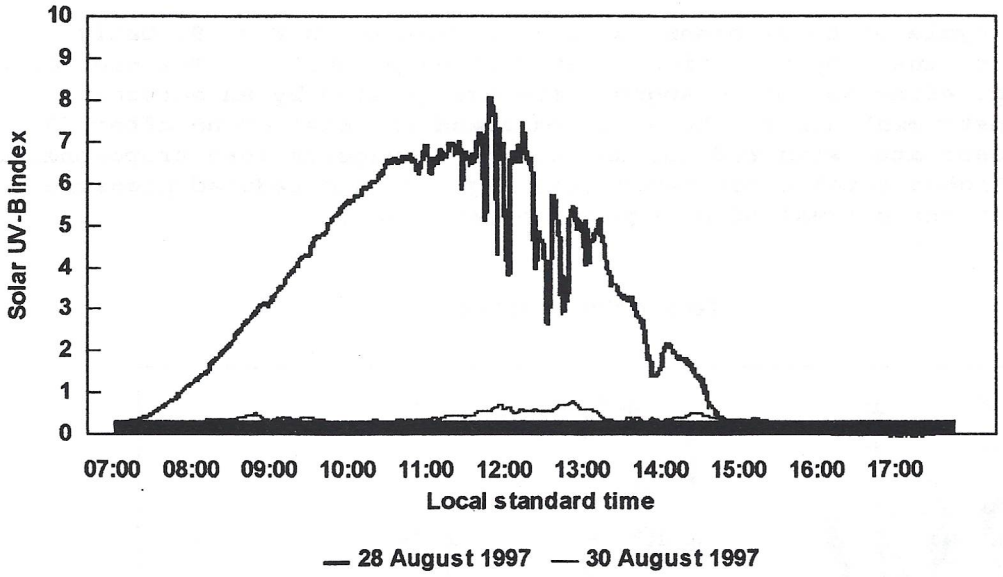


Fig. 8. Solar UV-B index on clearest (28 August) and smokiest (30 August) days at Alta Floresta. The peak UV-B index at solar noon at Seguin, Texas, is 10.1 to 11.3 for a similar air mass (1.06-1.07) and ozone column (263 to 270 Dobson units). The attenuation on 30 August exceeded the maximum attenuation measured at Cuiabá in 1995 during SCAR-B (Mims, 1996a).

Most visible and near-infrared total and diffuse radiation measurements have yet to be processed. These data will provide information about the spectral dependence of the diurnal diffuse/total irradiance at various optical depths. They will permit estimates of sub-canopy irradiance (Yanhong, *et al.*, 1996). They will provide information about the availability of the blue wavelengths that participate in photosynthesis and the phototropic response of plants and the far-red wavelengths that stimulate photosynthesis in purple bacteria and regulate seed germination. And negative spikes in the diurnal irradiance plots provide a record of when clouds were present at the Sun when smoke was too thick to see clouds.

## 2.3. Total Column Ozone

A Microtops II was configured as an ozonometer capable of measuring the total abundance of ozone in a column through the atmosphere. This instrument measured diurnal increases in total ozone associated with increases in optical depth. Some of the increase is apparently caused by aerosol-induced error, The remainder of the increase is caused by the significant increase in tropospheric ozone which has been observed to occur in previous studies of biomass burning in Brazil (e.g. SCAR-B in 1995).

### 2.3.1. Total Ozone Measurement Methodology

Total ozone was measured every 15 minutes. Prior to each measurment the instrument's window was checked for foreign matter and cleaned if necessary. Measurements were postponed when it appeared that the Sun was blocked by a cloud. (Clouds were often obscured by smoke.)

### 2.3.2. Total Ozone Measurement Results

The diurnal cycle of total ozone is clearly visible in Fig. 9. Daily increases are caused by pollution related ozone production. The high ozone amounts (e.g. afternoon of 30 August) are exaggerated by an aerosol dependent instrument error. The downward trend in total ozone after 30 August is associated with reduced smoke, which suggests less tropospheric ozone, and higher total water vapor (see Fig. 10) and reduced pressure, which suggest the arrival of an equatorial air mass.

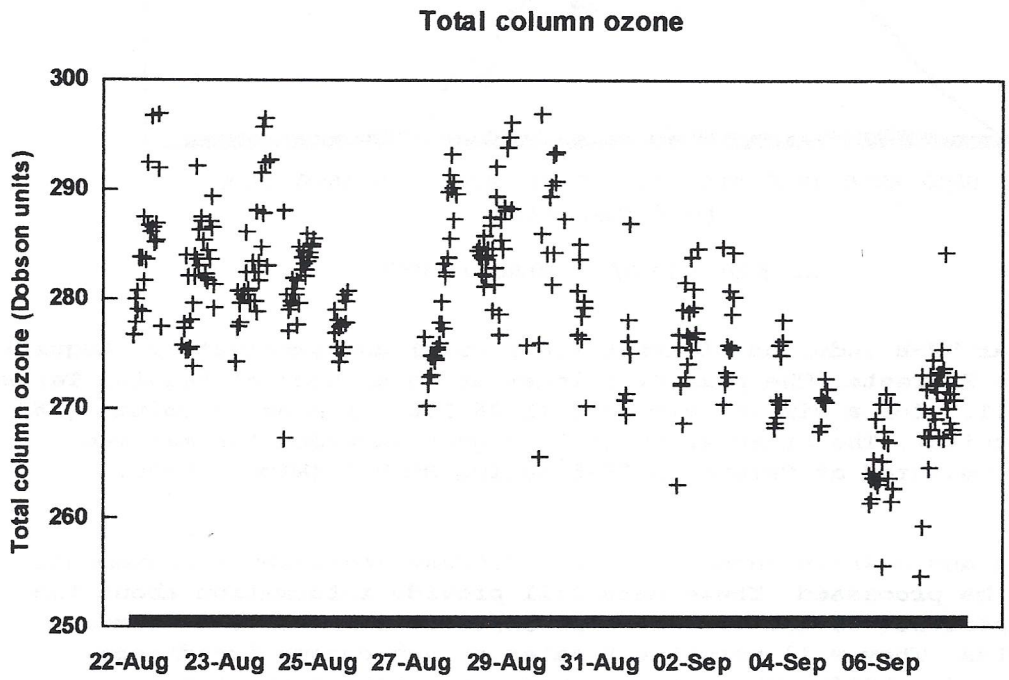


Fig. 9. Plotted are all total ozone measurements made at Alta Floresta and the Cristalino River site.

## 2.4. Total Column Water Vapor (Precipitable Water)

One of the Sun photometers (Microtops II) was configured as a near-infrared hygrometer capable of measuring the total abundance of ozone in a column through the atmosphere. (This instrument also measured total ozone.) Typical column water abundances ranged between about 2 and 3.2 cm.

### 2.4.1. Total Column Water Vapor Measurement Methodology

Total column water vapor was measured every 15 minutes (on the hour, quarter hour, etc.). Prior to each measurement the instrument's window was checked for foreign matter and cleaned if necessary. Measurements were postponed when it appeared that the Sun was blocked by a cloud. (Clouds were often obscured by smoke.)

### 2.4.2. Total Column Water Vapor Measurement Results

An upward trend in total column water vapor can be seen in Fig. 10. This increase is associated with lower total ozone (see Fig. 9) and reduced pressure, all of which imply the arrival of an equatorial air mass. Some of the diurnal increases on some days might be slightly exaggerated due to the instrument's aerosol dependence. The only significant rainfall occurred after sunset on 7 September and at 0300 on 8 September.

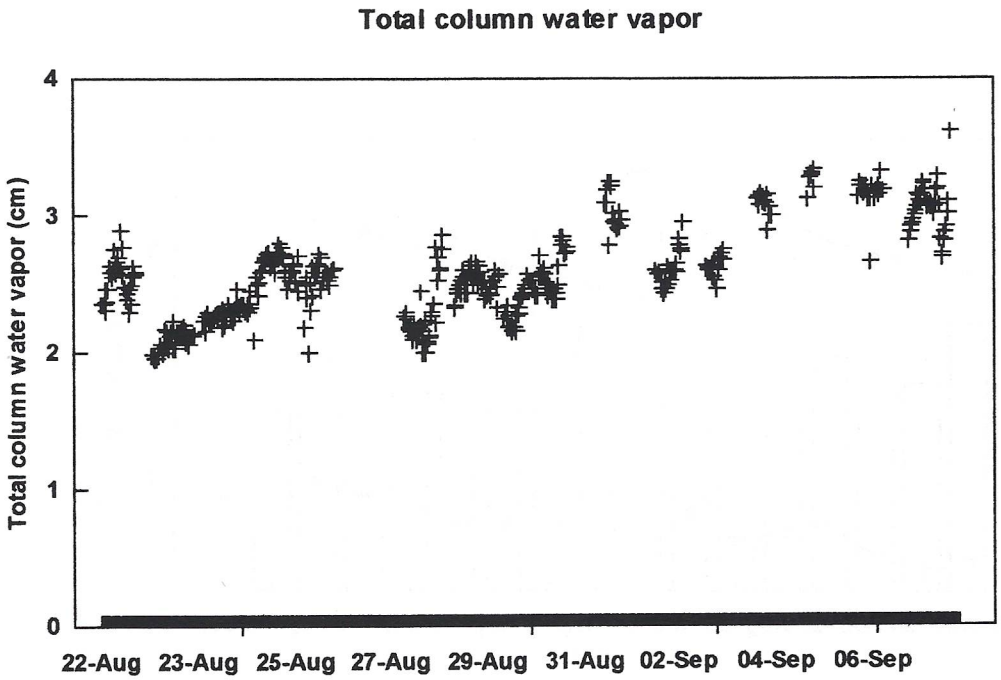


Fig. 10. Plotted are all the total column water vapor measurement made at Alta Floresta and the Cristalino River site.

## 2.5. Diurnal Temperature and Optical Depth

**The ambient temperature was measured at 1-minute intervals by a miniature Onset data logger placed in an open space sheltered by a concrete roof. There was a high correlation (r^2 = 0.83) of the peak daily temperature and photosynthetic photon flux during the 8-day period in which a small garden was raised. In view of the relative stability of the local weather during this period, it is reasonable to ascribe the measured**

### 2.5.1. Temperature Measurement Methodology

**Temperature was measured continuously during the entire stay at Alta Floresta by means of a miniature data logger (Onset Computer Corp.). From 22 August to 1 September, the temperature was logged every 60 seconds. This schedule required that the logger be downloaded each evening. From 2 to 5 September the temperature was logged every 192 seconds as the experimenter was at the Cristalino River site and the logger could not be downloaded each day. The temperature logger was placed on a wood surface about 20 cm under a concrete roof over an open air courtyard.**

### 2.5.2. Temperature Measurement Results

**Figure 11 shows the aerosol optical thickness (540 nm) at solar noon and the maximum and minimum daily temperature. The most obvious feature of this plot is that the lowest maximum temperature occurred on 30 August, the day with the highest AOT. Similarly, the highest maximum temperature occurred on 28 August, the day with the lowest AOT.**

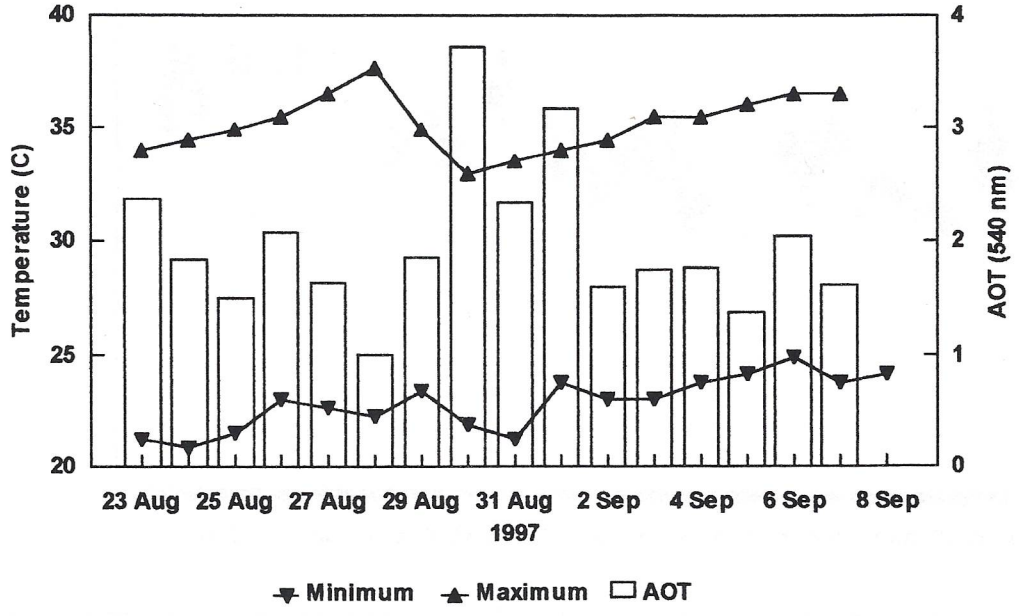


**Fig. 11. Daily optical depth (540 nm) at solar noon and maximum and minimum temperature for each day at Alta Floresta and the Cristalino River site.**

A comparison of the daily mean AOT and the maximum daily temperature suggests a possible cause and effect relationship. The linear regression line drawn through the points in the scatter graph in Figure 12 yields an r^2 of 0.71. The comparison is for 23 August to 1 September. Thereafter most observations were made at the Cristalino River site.

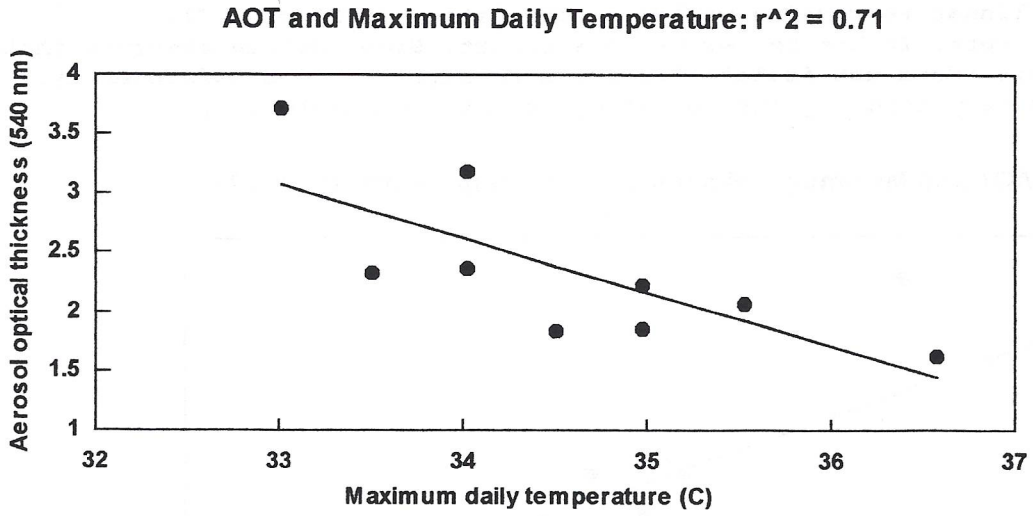


Fig. 12. Comparison of mean AOT at solar noon and the maximum daily temperature.

The daily heating rate is influenced by fluctuations in AOT, especially since AOT is usually greater in mid-afternoon than in the morning. The total photosynthetic flux was measured on 7 days at Alta Floresta, and a comparison of total PAR with the maximum daily temperature yields an r^2 = 0.83 (Fig 13). This comparison does not consider possible weather effects.

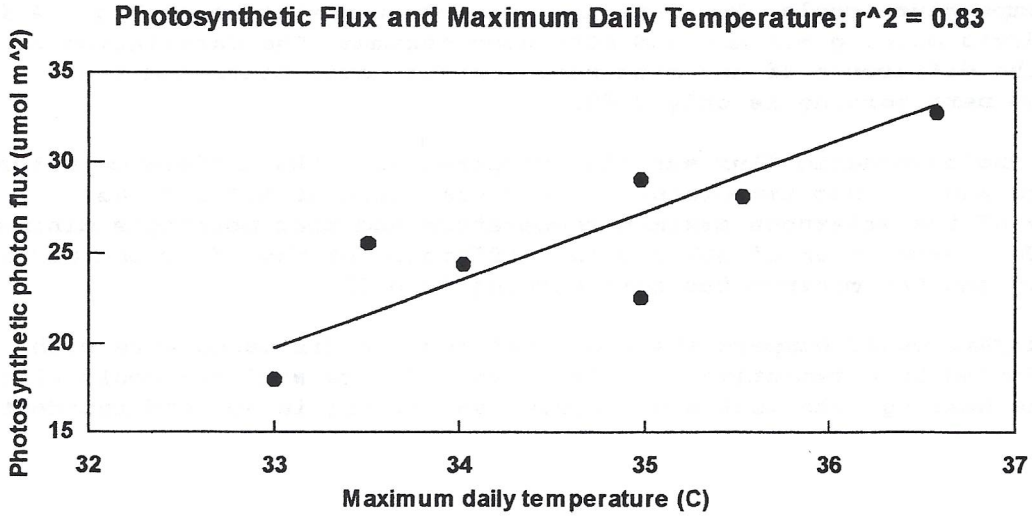


Fig. 13. Comparison of the daily total photosynthetic photon flux and the maximum daily temperature.

The clearest time of day at Alta Floresta was generally early morning. Nevertheless, considerable smoke was present during the night. Although no measurements were made, the smoke could be clearly seen in the beams of a small laser and a flashlight. Smoke usually obscured all but one planet and possibly a few stars. To determine if the presence of aerosols at night influenced nocturnal cooling, the mean daily AOT was compared with the difference between the maximum and minimum daily temperature. As shown in Fig. 14, a linear regression yields a correlation (r^2) of 0.71. (Reviewer's Note: In his review of this report, Brent Holben observes that this analysis "does not isolate the issue of night cooling sufficiently, since ΔT is very strongly influenced by maximum temperature.")

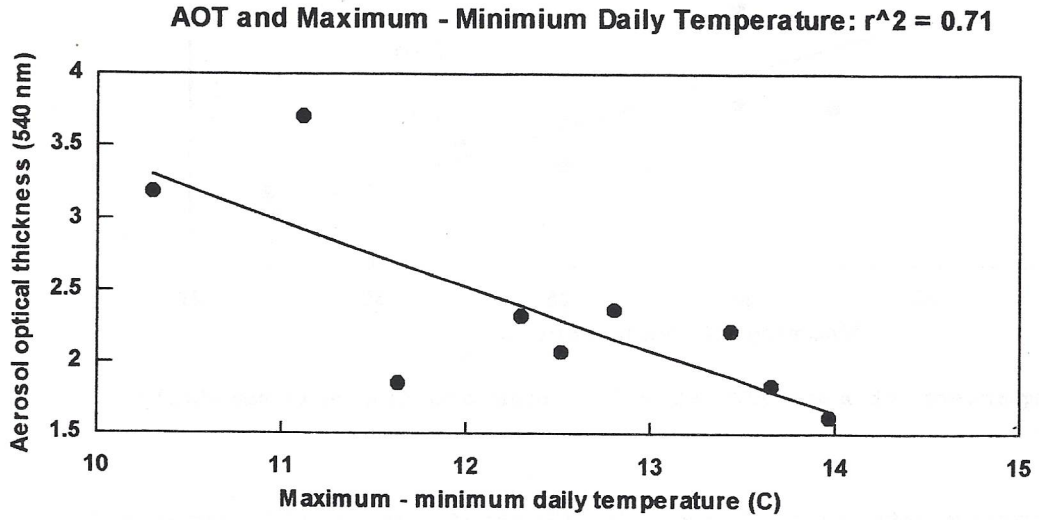


Fig. 14. Comparison of mean AOT at solar noon and the difference between the daily maximum and minimum temperature.

The comparison in Fig. 14 suggests a possible association of AOT and the diurnal temperature cycle. The maximum - minimum temperature in Fig. 14 is the same day's morning minimum and afternoon maximum. The correlation of AOT with the difference of the afternoon maximum temperature and the minimum the next morning is only 0.40.

The total photosynthetic flux was also compared with the difference between the maximum and minimum temperature. The correlation of AOT and the difference of the afternoon maximum temperature and that morning's minimum is 0.56. The correlation of AOT and the difference of the afternoon maximum temperature and the minimum the next morning is 0.51.

Future analysis could compare the empirical results discussed here with those predicted by a radiative transfer model. Future analysis could also compare the heating rate with simultaneous variations in AOT and incident PAR.

## 2.6. Comparison of Surface and Satellite Observations

The Total Ozone Mapping Spectrometer (TOMS) has served as NASA's principle ozone retrieval satellite instrument since 1978. Besides providing high quality measurements of the global distribution of ozone, this remarkable instrument can also monitor sulfur dioxide from volcanic eruptions (Krueger, 1983) and aerosols (Herman *et al.*, 1997). TOMS ozone amounts can also be used in various models that estimate the surface UV-B. These new applications of TOMS data suggest a possible role for TOMS as an epidemiological tool for the identification of regions with unusually high and low levels of UV-B.

During SCAR-B in 1995, a comparison of TOMS and surface measurements was not possible as METEOR-3 TOMS had failed. During the present study, EarthProbe TOMS was in orbit. However, the low altitude of this satellite limited coverage to two of every 3 days. Fortunately, TOMS coverage was available on 30 August, the day with highest optical depth. But TOMS coverage was not available on 28 August, the day with the lowest optical depth.

### 2.6.1. TOMS Aerosol Index and Surface AOT at Alta Floresta

Figure 15 is a scatter plot that compares the preliminary aerosol index measured by EarthProbe TOMS (331 nm/360 nm) and the aerosol optical thickness (AOT) at 376 nm measured by a SUNTOPS Sun photometer.

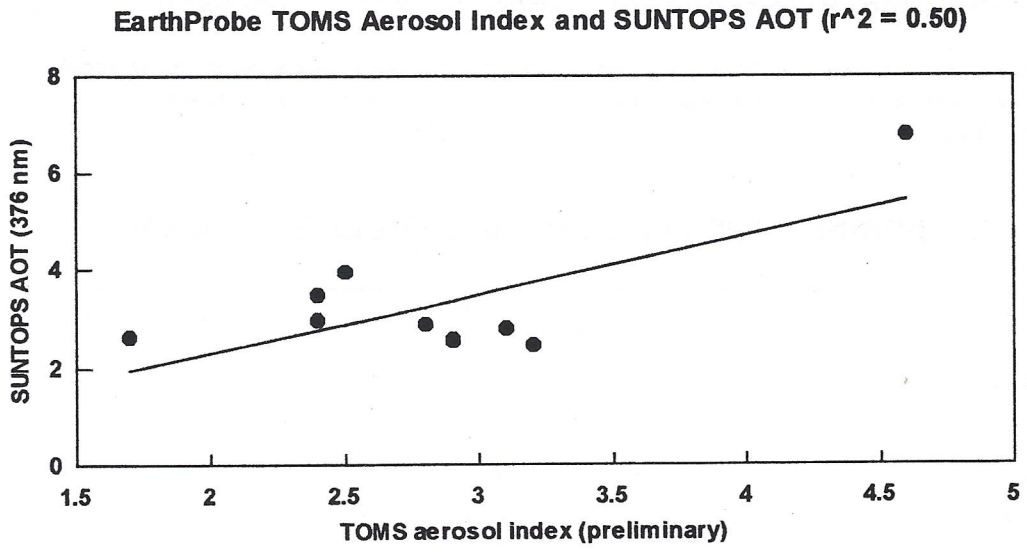


Fig. 15. Scatter plot of aerosol index measured by EarthProbe TOMS and the AOT at 376 nm measured by a SUNTOPS Sun photometer at Alta Floresta, Brazil. The number of points is limited by the 2 of 3 day coverage of the satellite.

## 2.6.2. TOMS Aerosol Index and Surface UV-B at Alta Floresta

**Measurements of the aerosol index by TOMS and the surface UV-B at Alta Floresta were weakly correlated (r^2 = 0.54). More measurements under a wider range of aerosol conditions and inclusion of ozone absorption are required to better compare these parameters.**

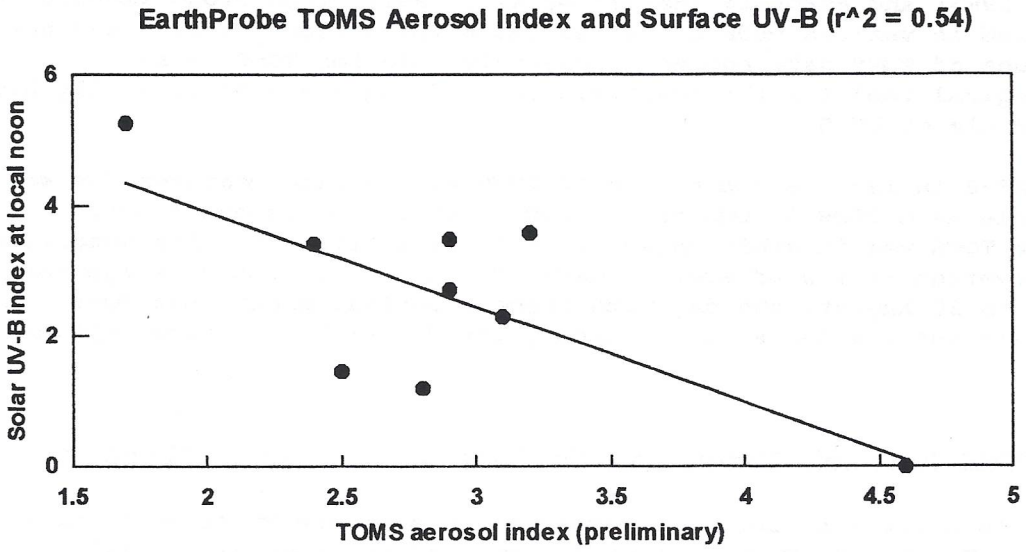


**Fig. 16. Aerosol index measured by EarthProbe TOMS and the surface UV-B.**

## 2.6.3. TOMS and Microtops II Ozone at Alta Floresta

**Total ozone measured by TOMS and Microtops II was poorly correlated, probably because of severe aerosol loading and aerosol dependent error of Microtops II.**

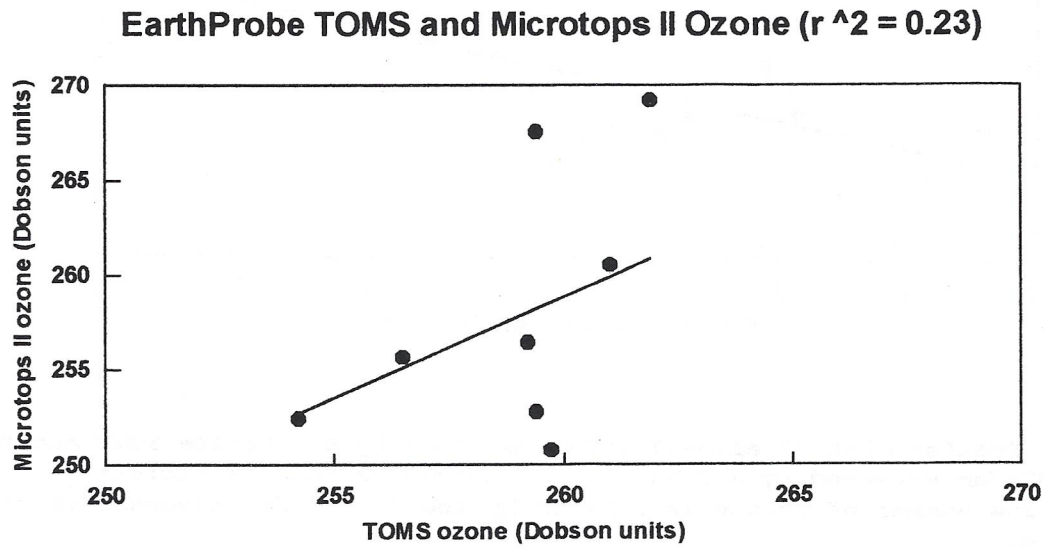


**Fig. 17. Total ozone measured by EarthProbe TOMS and Microtops II.**

# 3. BIOLOGICAL STUDIES AND EXPERIMENTS

Several biological studies were conducted in Alta Floresta simultaneous with the gathering of Sun and atmospheric data. The results of these studies suggest that additional biological studies in regions with severe aerosol loading are warranted.

## 3.1. Airborne Bacteria and UV-B

Excessive UV-B can suppress the growth of certain plants, enhance the growth of plants whose predators are suppressed by UV-B (Bothwell *et al.*, 1994) and cause immune suppression, eye damage and various cancers in people. Very low levels of UV-B can cause the development of rickets (Galindo et al., 1995), increase the number of nursery sites for UV-sensitive mosquitoes (Mims, 1997a) and possibly increase the survival of pathogenic bacteria and viruses suspended in air and water (Mims *et al.*, 1997b, Mims, 1997c). UV-B in natural sunlight suppresses bacteria in drinking water that cause diarrhea in African children (Conroy, 1996).

The principle biological study was the collection of airborne bacteria. Solar UV-B has been shown to select for pigmented bacteria in the outdoor ambient atmosphere (Tong and Lighthart, 1997), and severe aerosol loading caused by smoke in Brazil significantly reduces solar UV-B (Mims, 1995b & 1996c). The proposal for this research stated, "Infectious disease may be enhanced by the diminishment of normal levels of bactericidal levels of UV-B in severely polluted regions. This experiment will determine if severe air pollution enhances the number of non-pigmented airborne bacteria." As Fig. 18 shows, this clearly was the case.

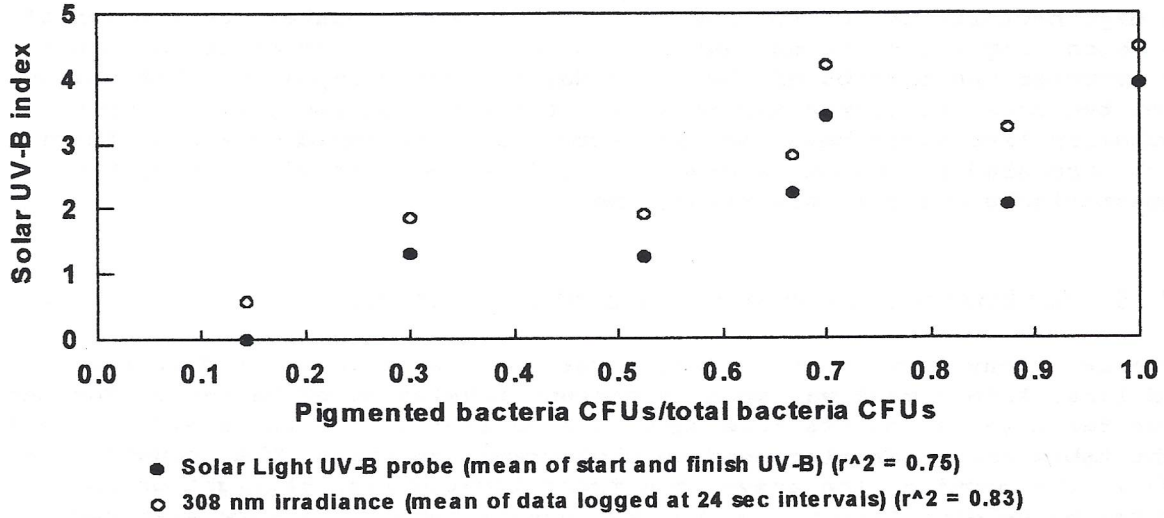


Fig. 18. Total solar UV-B and the ratio of pigmented to total count bacteria at solar noon from 25 August to 2 September 1997 at Alta Floresta, Brazil. UV-B was measured with two instruments. A Solar Light probe adjacent to the agar tray measured UV-B at the beginning and end of each 30-minute exposure. A 308-nm probe 60 meters ESE of the agar tray sampled UV-B at 24-second intervals. The mean of the measured UV-B is plotted for both instruments.

### 3.1.1. Airborne Bacteria Collection

Airborne bacteria were collected in the open air using pre-prepared, sterile agar trays (Biotest Hycon total count contact slides). The manufacturer lists the culture medium ingredients per liter of distilled water as pancreatic digest of casein (15.0 g), soy bean peptone (5.0 g), sodium chloride (5.0 g), lecithin (0.7 g), polysorbate 80 (7.0 g), L-histidine (1.0 g) and agar-agar (17.0 g). Representative agar was tested by the manufacturer according to SOP # SV-D:QK-5057-00, and the medium was found to be sterile after 7 days incubation at 22 C and 32 C. All trays were visually inspected before use, and none showed evidence of contamination. The manufacturer reports "good" growth results using various bacteria, including *Staphylococcus aureas, Escherichia coli, Bacillus subtillis, Aspergillus niger, Candida albicans* and *Pseudomonas aeruginosa*.

On 7 consecutive days, an agar tray was placed on a wood post 1.5 meters above the ground with full sunlight exposure at 6 times during the day (approximately 0700, 1030, 1200, 1430, 1700, and 2230 hours) for about 30 minutes. Insect repellant was sprayed around the top of the post to discourage insects. Wind speed and solar UV-B were measured with a Kestrel air speed indicator and a calibrated Solar Light probe immediately before and after the agar tray was exposed to air. UV-B was also measured at 24 second intervals by a data logger on a roof 40 meters SE of the agar tray. To save agar trays for use at a rain forest site, bacteria were sampled at only solar noon on several days following the 7 consecutive days.

### 3.1.2. Airborne Bacteria Incubation

Agar trays were visually inspected and then inserted in their carriers immediately after exposure to the ambient air. Exposed agar trays were incubated in darkness at ambient temperature for 24-48 hours. For the first few days bacteria colony forming units (CFUs) were counted the evening of the second day following exposure. CFUs collected on and after 25 August were counted the morning of the third day following exposure. This change permitted more CFU growth and more rest for the experimenter. A longer incubation time would have been preferred. But the rapid growth of fungi, which concealed the bacteria CFUs with a dense network of white hyphae, necessitated a briefer incubation time.

### 3.1.3. Airborne Bacteria CFU Counting Method

Bacteria colony forming units (CFUs) were counted with the aid of a x10 hand lens. A face mask was worn to prevent inhalation of bacteria. For the first few days the counts were made by backlighting the trays with a small light table which was also used to photograph the trays. When counts were made in the morning, the trays were front lighted with skylight or back lighted by holding them up to the sky. Questionable CFUs were examined using both methods. The number of CFUs on a single agar tray ranged from 0 (usually at night) to 52.

CFUs which superficially resembled mold and fungus were not counted. After the total count was made, a second count of only the pigmented CFU's was made. CFUs with any hue other than clear, white or gray were classified as pigmented. The most common pigmented CFUs were orange or yellow (one pink colony, superficially similar to *Serratia marcescens*, was observed).

At least two slides were contaminated by insects (ant and small grasshopper) during exposure to outdoor air. Colonies in the contaminated regions of these two slides were not counted. Most of the orange and yellow CFUs superficially resemble those which grew on a contact slide pressed against the dorsal side of a leaf on a small tree 12.5 meters ESE of the collection point. It is instructive that while 82% of the CFUs collected on the dorsal, sunny side of this leaf were pigmented (orange), only 7% of the CFUs collected from the ventral, shaded side of the same leaf were pigmented (Fig. 19). The tracks of at least one flying insect and an ant were indicated by orange CFUs similar in appearance to most airborne CFUs and CFUs collected on the leaf. Other pigmented and non-pigmented CFUs have a wide range of physical appearances, thus indicating a variety of bacteria.

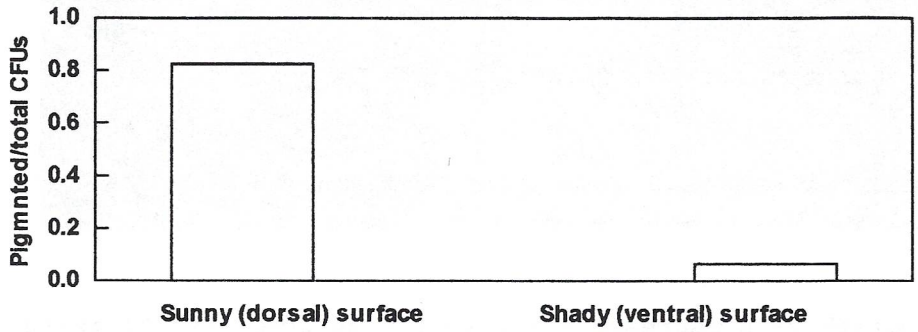


Fig. 19. Ratio of pigmented to total CFUs on sunny and shady sides of a living tree leaf 12.5 meters from the bacteria collection point.

### 3.1.4. Bacteria CFU Photography Method

The agar trays were photographed immediately after the counting procedure. The date and exposure time for each tray was printed on transparent tape, and trays were then taped to a portable light table. Photographs were made with a Pentax Super Program with a 50-mm macro lens with an aperture setting of f/11 and an exposure time of 0.25 second. All photographs were made on Kodak Kodacolor 100 film (ISO 100) with the same expiration date. Representative photograph of CFUs on agar trays are shown in the accompanying color plates.

### 3.1.5. Safe Disposal of Exposed Agar Trays

Two methods were used to disinfect and dispose of exposed agar trays. In Alta Floresta, a commercial swimming pool disinfectant was mixed with water in a plastic container (from the greenhouse). Exposed agar trays were soaked in the solution and placed in a plastic bag. The bag was marked with precautionary wording in both English and Portuguese. Agar slides exposed at rain forest sites on the Cristalino River were disinfected using a commercial spray disinfectant (Lysol) brought to Brazil for this purpose. Instruments, surfaces and hands which came in close proximity or touched the agar trays were disinfected with the commercial spray disinfectant. No exposed agar trays were carried into or out of Brazil.

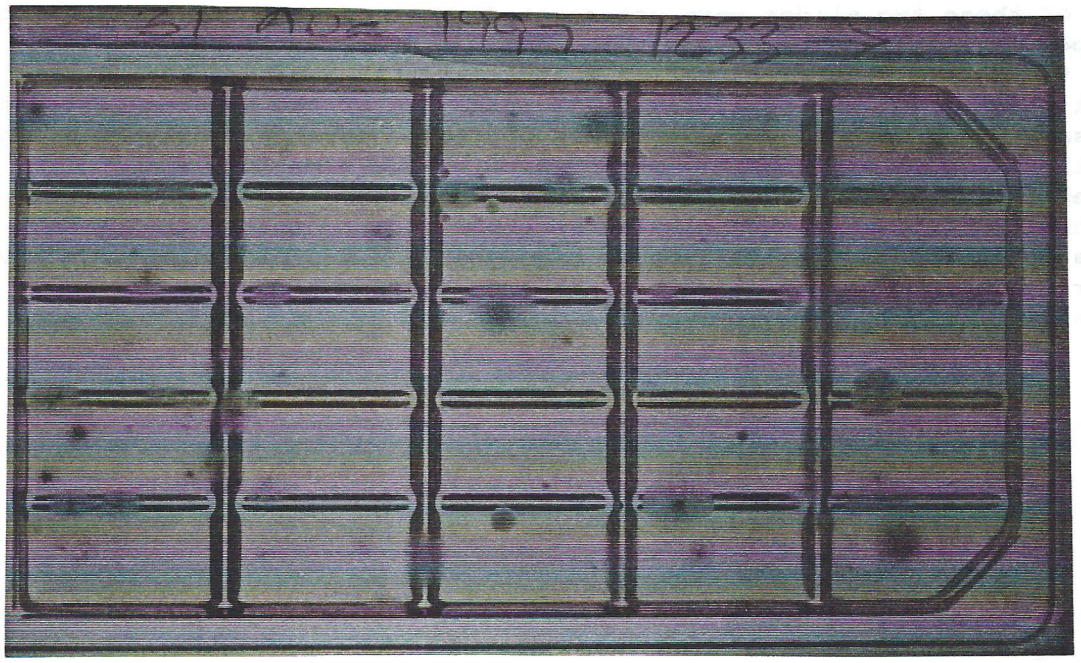


**Plate 1. Photograph of a representative agar tray from Alta Floresta (31 August 1997, 1233 hrs). Most of the distinctly round colonies are bacteria. The diffuse white and dark colonies are molds.**

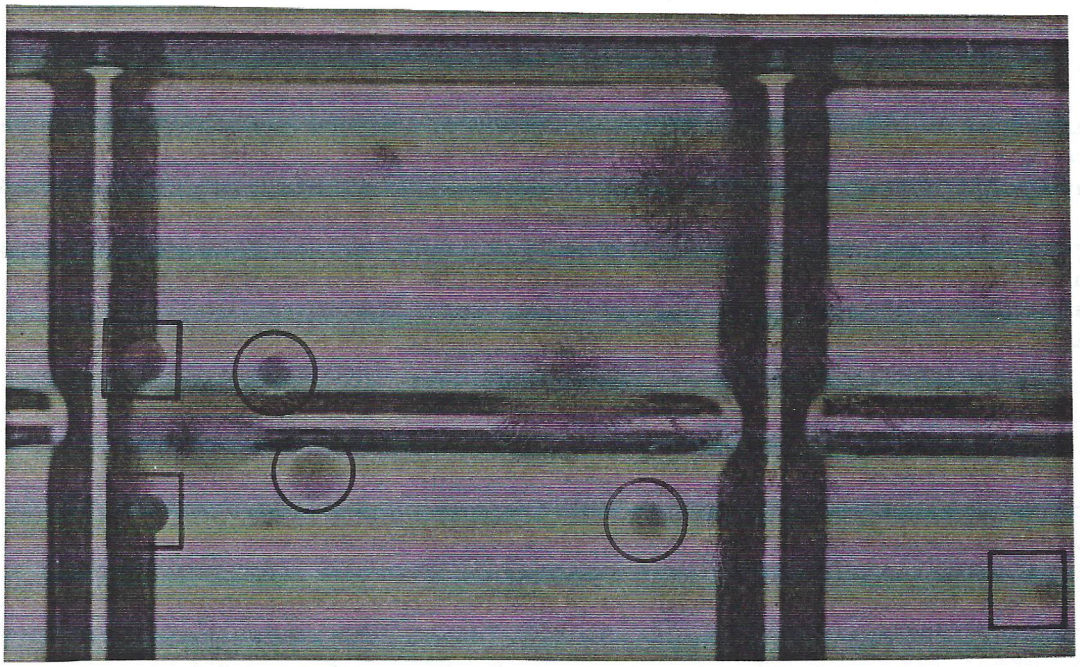

**Plate 2. Enlarged view of the upper-center portion of the tray in Plate 1 showing orange-pigmented bacteria colonies (circles) and non-pigmented**

## 3.1.6. Results of Airborne Bacteria Study

Prior to the study in Alta Floresta, the findings of Tong and Lighthart (1996) regarding the relationship of solar UV-B to the ratio of pigmented to non-pigmented bacteria CFUs were informally tested at the investigator's facility in South-Central Texas. Tong and Lighthart employed commercial samplers to collect airborne bacteria. No such sampling devices were available for the informal test. Instead, airborne bacteria were collected using the agar tray method described above. Since the ratio of the bacteria types is at issue, an absolute count, while desirable, is not required. The results of the informal test were very similar to the findings of Tong and Lighthart. Therefore the methodology of the informal test was used for the study at Alta Floresta.

Figure 20 is a summary of the airborne bacteria study at Alta Floresta. Though the standard deviations are large for the noon and afternoon CFU counts, the trend is very similar to that observed by Tong and Lighthart in Oregon (1996) and in Texas (Mims, unpublished).

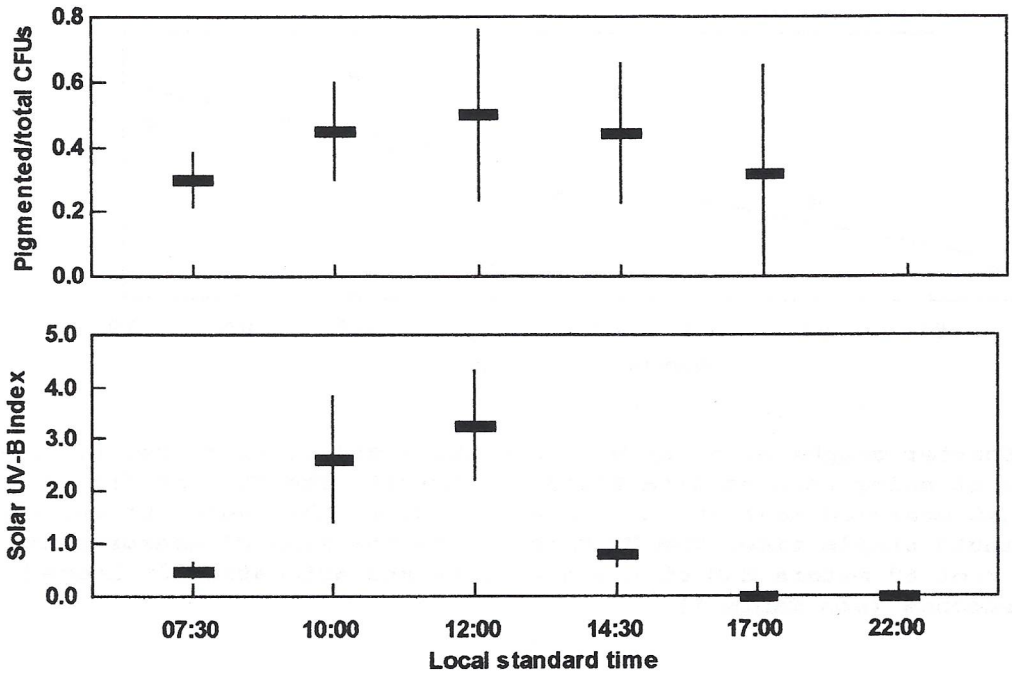


Fig. 20. The upper plot shows the mean (horizontal bar) and the standard deviation (vertical line) of the ratio of pigmented to total count bacteria CFUs during 30-minute sample times on 22 to 28 August 1997 at Alta Floresta. The lower plot shows the mean and the standard deviation of the mean of the daily total-sky solar UV-B index during the times bacteria were being collected. The UV-B was measured with a 308-nm detector (10 nm FWHM) and stored in a miniature data logger at 24-second intervals.

Figure 21 shows the ratio of pigmented to total count bacteria CFUs and the total UV-B measured with a Solar Light UV-B probe (a) and a data logging UV-B probe (b) (Mims & Fredrick, 1994).

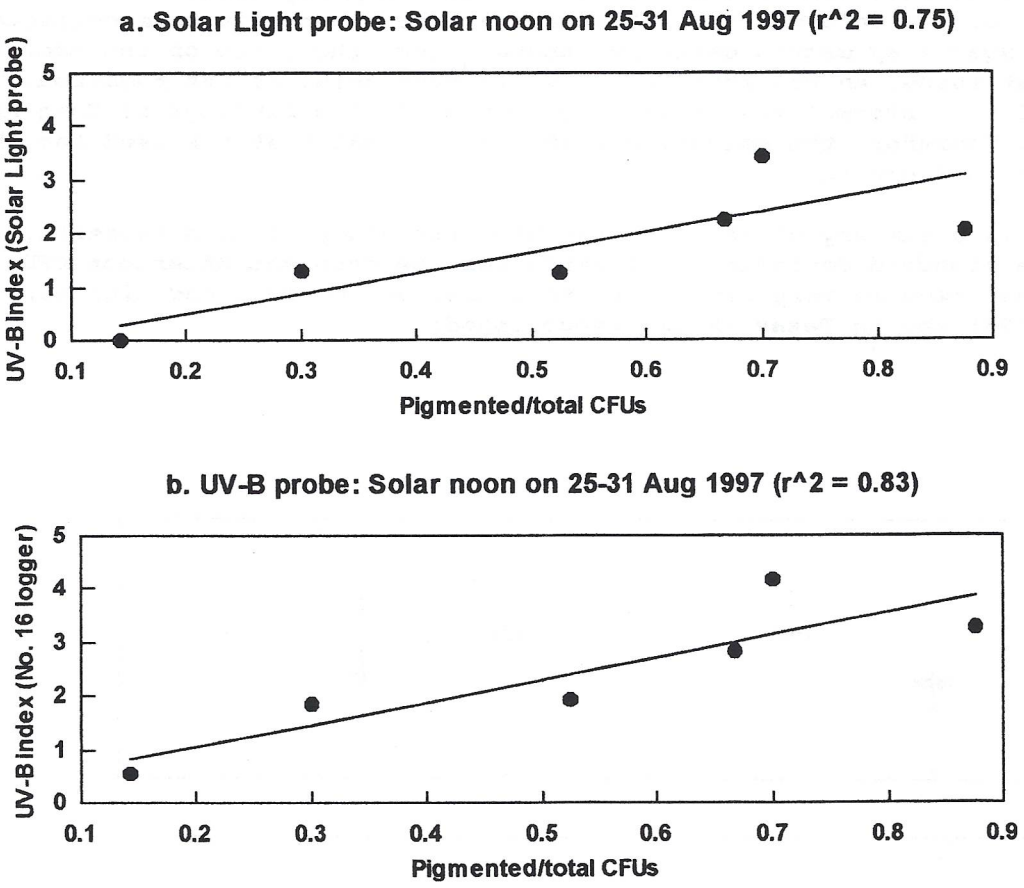


Fig. 21. Scatter graphs of solar UV-B and the ratio of pigmented to total count CFUs at solar noon at Alta Floresta, Brazil. The UV-B in (a) is the mean of that measured adjacent to the agar tray at the beginning and end of each 30-minute sample time. The UV-B in (b) is the mean of measurements made on a roof 60 meters ESE of the agar tray and automatically logged every 24 seconds (see Table 1).

Tong and Lighthart (1997) have shown that pigmented bacteria are more resistant to solar UV-B than non-pigmented types and that the ratio of pigmented to non-pigmented types increases at solar noon during a 4-day study. These results are confirmed by the observations in Alta Floresta, as the present study shows a high correlation ($r^2 = 0.83$) of solar UV-B and the ratio of pigmented to non-pigmented bacteria CFUs. As many pathogenic bacteria are non-pigmented, their population may be enhanced by the sharply reduced UV-B in biomass burning regions. The implications of this finding for the measured increase in infectious disease observed in biomass burning regions deserves further study.

| Bacteria Colony Forming Unit | | | OK | | | Wind | Wind | Wind | UV-B | UV-B | UV-B |
|---|---|---|---|---|---|---|---|---|---|---|---|
| 22 August 1997 | | | | | | Start | Stop | Mean | Start | Stop | Mean |
| Start | Stop | Total | Non-Pigment | Pigment | Ratio | (m/sec) | (m/sec) | (m/sec) | | | |
| 07:33 | 08:03 | 48 | 33 | 15 | 31% | 0.3 | 0.5 | 0.4 | 0.3 | 0.5 | 0.4 |
| 10:00 | 10:30 | 24 | 12 | 12 | 50% | 0 | 0.9 | 0.45 | 2.2 | 2.9 | 2.55 |
| 12:00 | 12:30 | 4 | 2 | 2 | 50% | 1.1 | 1.2 | 1.15 | 2.5 | 1.7 | 2.1 |
| 14:33 | 15:03 | 4 | 2 | 2 | 50% | 1 | 0.4 | 0.7 | 1 | 0.3 | 0.65 |
| 17:00 | 17:30 | 3 | 0 | 3 | 100% | 0.2 | 0.7 | 0.45 | 0 | 0 | 0 |
| 22:00 | 22:30 | 0 | 0 | 0 | ERR | 0.1 | 0 | 0.05 | 0 | 0 | 0 |

| Bacteria Colony Forming Unit | | | OK | | | Wind | Wind | Wind | UV-B | UV-B | UV-B |
|---|---|---|---|---|---|---|---|---|---|---|---|
| 23 August 1997 | | | | | | Start | Stop | Mean | Start | Stop | Mean |
| Start | Stop | Total | Non-Pigment | Pigment | Ratio | (m/sec) | (m/sec) | (m/sec) | | | |
| 08:08 | 08:50 | 25 | 22 | 3 | 12% | 0.40 | 0.60 | 0.5 | 0.5 | 0.8 | 0.65 |
| 10:02 | 10:32 | 7 | 4 | 3 | 43% | 0.20 | 0.10 | 0.15 | 1.3 | 1.1 | 1.2 |
| 12:00 | 12:30 | 24 | 16 | 8 | 33% | 0.60 | 0.40 | 0.5 | 2.5 | 2.6 | 2.55 |
| 14:02 | 14:39 | 8 | 7 | 1 | 13% | 0.00 | 0.50 | 0.25 | 1 | 0.8 | 0.9 |
| 17:10 | 17:44 | 17 | 10 | 7 | 41% | 0.20 | 0.10 | 0.15 | 0 | 0 | 0 |
| 22:02 | 22:32 | 3 | 3 | 0 | 0% | 0.20 | 0.30 | 0.25 | 0 | 0 | 0 |

| Bacteria Colony Forming Unit | | | OK | | | Wind | Wind | Wind | UV-B | UV-B | UV-B |
|---|---|---|---|---|---|---|---|---|---|---|---|
| 24 August 1997 | | | | | | Start | Stop | Mean | Start | Stop | Mean |
| | | Total | Non-Pigment | Pigment | Ratio | (m/sec) | (m/sec) | (m/sec) | | | |
| 07:55 | 08:28 | 8 | 6 | 2 | 25% | 0.2 | 0.2 | 0.2 | 0.3 | 0.5 | 0.4 |
| 10:03 | 10:38 | 5 | 3 | 2 | 40% | 1.7 | 1.5 | 1.6 | 2 | 2.4 | 2.2 |
| 12:03 | 12:59 | 6 | 3 | 3 | 50% | 0.6 | 0.3 | 0.45 | 2.8 | 2.9 | 2.85 |
| 14:34 | 15:10 | 7 | 5 | 2 | 29% | 0.4 | 0 | 0.2 | 1.1 | 0.75 | 0.925 |
| 16:56 | 17:30 | 6 | 5 | 1 | 17% | 0.5 | 0 | 0.25 | 0.1 | 0 | 0.05 |
| 22:02 | 22:34 | 1 | 1 | 0 | 0% | 0.3 | 0 | 0.15 | 0 | 0 | 0 |

| Bacteria Colony Forming Unit | | | OK | | | Wind | Wind | Wind | UV-B | UV-B | UV-B |
|---|---|---|---|---|---|---|---|---|---|---|---|
| 25 August 1997 | | | | | | Start | Stop | Mean | Start | Stop | Mean |
| Start | Stop | Total | Non-Pigment | Pigment | Ratio | (m/sec) | (m/sec) | (m/sec) | | | |
| 07:23 | 08:18 | 16 | 11 | 5 | 31% | 0 | 0 | 0 | 0.1 | 0.5 | 0.3 |
| 10:18 | 10:38 | 7 | 3 | 4 | 57% | 1 | 0 | 0.5 | 2.1 | 2.6 | 2.35 |
| 12:16 | 12:39 | 3 | 2 | 1 | 33% | 0.7 | 2.6 | 1.65 | 2.9 | 2.8 | 2.85 |
| 14:45 | 15:26 | 8 | 4 | 4 | 50% | 0.4 | 0.3 | 0.35 | 1.1 | 0 | 0.55 |
| 17:06 | 17:49 | 5 | 5 | 0 | 0% | 0.7 | 0.8 | 0.75 | 0 | 0 | 0 |
| 22:25 | 23:33 | 16 | 13 | 3 | 19% | 0 | 0.3 | 0.15 | 0 | 0 | 0 |

| Bacteria Colony Forming Unit | | | OK | | | Wind | Wind | Wind | UV-B | UV-B | UV-B |
|---|---|---|---|---|---|---|---|---|---|---|---|
| 26 August 1997 | | | | | | Start | Stop | Mean | Start | Stop | Mean |
| Start | Stop | Total | Non-Pigment | Pigment | Ratio | (m/sec) | (m/sec) | (m/sec) | | | |
| 07:27 | 08:14 | 9 | 6 | 3 | 33% | 0.2 | 0.4 | 0.3 | 0.3 | 0.6 | 0.45 |
| 09:39 | 10:16 | 16 | 12 | 4 | 25% | 0.4 | 0.7 | 0.55 | 1.7 | 2 | 1.85 |
| 12:24 | 13:03 | 8 | 7 | 1 | 13% | 0.5 | 0.8 | 0.65 | 2.4 | 3.3 | 2.85 |
| 14:49 | 15:27 | 17 | 5 | 12 | 71% | 1.1 | 0.1 | 0.6 | 1.4 | 0.8 | 1.1 |
| 17:12 | 17:47 | 6 | 5 | 1 | 17% | 0.7 | 0.4 | 0.55 | 0 | 0 | 0 |
| 22:27 | 23:08 | 3 | 3 | 0 | 0% | 0 | 0 | 0 | 0 | 0 | 0 |

| Bacteria Colony Forming Unit | | | OK | | | Wind | Wind | Wind | UV-B | UV-B | UV-B |
|---|---|---|---|---|---|---|---|---|---|---|---|
| 27 August 1997 | | | | | | Start | Stop | Mean | Start | Stop | Mean |
| Start | Stop | Total | Non-Pigment | Pigment | Ratio | (m/sec) | (m/sec) | (m/sec) | | | |
| 07:34 | 08:13 | 13 | 8 | 5 | 38% | 0.3 | 0.3 | 0.3 | 0.4 | 0.7 | 0.55 |
| 10:00 | 10:34 | 29 | 21 | 8 | 28% | 1.4 | 0.2 | 0.8 | 2.8 | 2.9 | 2.85 |
| 12:03 | 12:38 | 10 | 3 | 7 | 70% | 0.5 | 0.3 | 0.4 | 4.4 | 4 | 4.2 |
| 14:37 | 15:12 | 12 | 9 | 3 | 25% | 0.5 | 0.2 | 0.35 | 1.2 | 0.8 | 1 |
| 17:09 | 17:40 | 4 | 4 | 0 | 0% | 0.7 | 0.4 | 0.55 | 0 | 0 | 0 |
| 23:10 | 23:51 | 52 | 45 | 7 | 13% | 0.2 | 1 | 0.6 | 0 | 0 | 0 |

| Bacteria Colony Forming Units | | | | | | Wind | Wind | Wind | UV-B | UV-B | UV-B |
|---|---|---|---|---|---|---|---|---|---|---|---|
| 28 August 1997 | | | | | | Start | Stop | Mean | Start | Stop | Mean |
| Start | Stop | Total | Non-Pigment | Pigment | Ratio | (m/sec) | (m/sec) | (m/sec) | | | |
| 07:19 | 07:52 | 8 | 5 | 3 | 38% | 0.4 | 0.3 | 0.35 | 0.4 | 1 | 0.7 |
| 09:36 | 10:07 | 7 | 2 | 5 | 71% | 0.6 | 1.6 | 1.1 | 4.7 | 5.9 | 5.3 |
| 12:19 | 12:52 | 15 | 0 | 15 | 100% | 3 | 1.4 | 2.2 | 4.9 | 5.9 | 5.4 |
| 14:37 | 15:21 | 11 | 3 | 8 | 73% | 0 | 0.3 | 0.15 | 0.6 | 0.3 | 0.45 |
| 17:12 | 17:47 | 4 | 2 | 2 | 50% | | | ERR | | | ERR |
| 22:27 | 23:08 | 2 | 2 | 0 | 0% | | | ERR | | | ERR |

**Table 1. Airborne bacteria experiment results (UV-B: Solar Light probe).**

## 3.2. Photosynthetic Active Radiation (PAR)

Measurements by Cimel Sun photometers (Holben *et al.*, 1996) and miniature radiometers (Mims & Frederick, 1994) in Brazil during SCAR-B in 1995 showed significant reductions in photosynthetic active radiation (PAR) during episodes of severe aerosol loading caused by smoke. PAR was reduced significantly at Alta Floresta during the present study.

### 3.2.1. PAR Measurement Methodology

PAR was measured with an Apogee detector calibrated against a Licor PAR detector. The Apogee detector was connected to a data logger. Photosynthesis is most efficient at red and blue wavelengths, and the Apogee detector detects red wavelengths with much greater efficiency than blue wavelengths. This is not a major drawback under most conditions. However, smoke aerosols absorb blue wavelengths much more efficiently than red wavelengths, thus causing the Apogee detector to overestimate the available PAR at Alta Floresta, especially on the smokiest days.

### 3.2.2. Results of PAR Measurements

The clearest and smokiest days at Alta Floresta occurred on, respectively, 28 and 30 August. Figure 22 shows the PAR on these days.

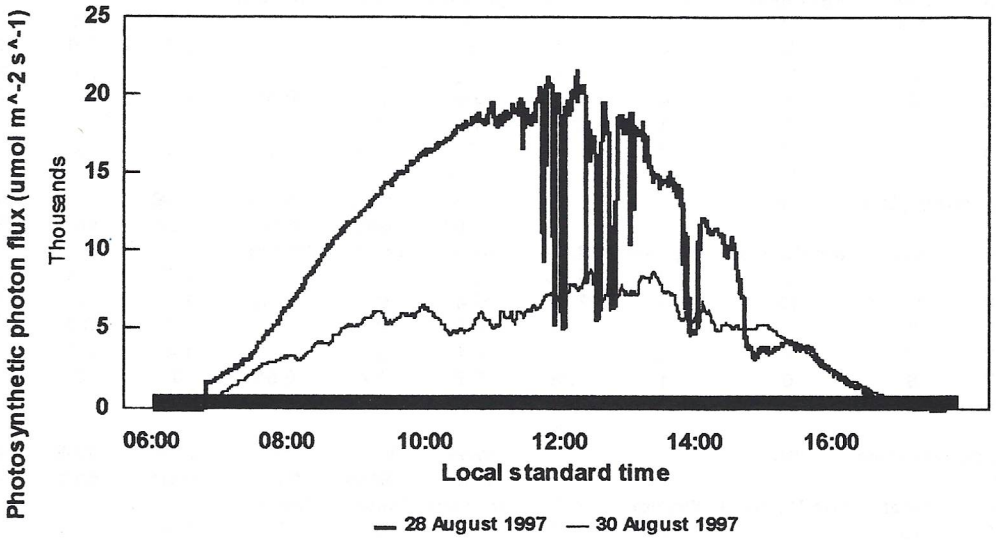


Fig. 22. Total photosynthetic photon flux on the clearest (28 August) and smokiest days (30 August) at Alta Floresta. The negative spikes after 12:00 hours on 28 August were caused by cumulus clouds passing before the Sun.

The daily photosynthetic photon flux at mid-latitudes in summer ranges from 30 to 60 mol m-2 (Bugbee and Monje, 1992), and the production of biomass by certain field crops (e.g. wheat) is linear with respect to PAR (Bugbee and Salisbury, 1988). The mean flux at Alta Floresta (25 Aug to 1 Sep) was 27.4 mol m-2 (standard error of 6 mol m-2), with the highest and lowest days being 38.8 and 17.9 mol m-2, respectively. In short, severe aerosol loading caused by biomass burning reduces the mean daily PAR at this tropical site to slightly below the lower limit of daily PAR at a mid-latitude site.

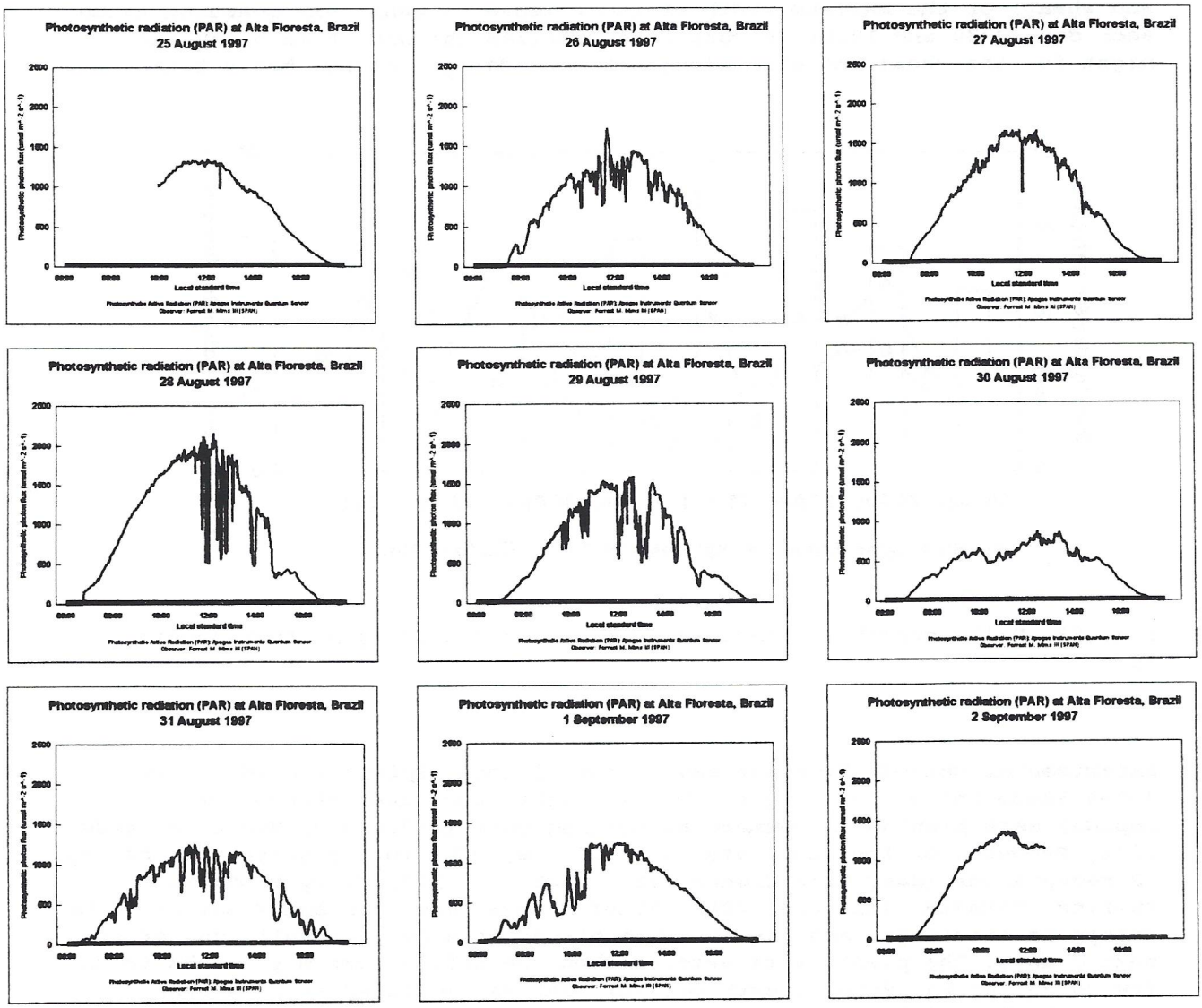


**Fig. 22 (a). Total photosynthetic photon flux measured during the miniature garden experiment described in 3.2.3. Note the wide range of PAR during this period.**

## 3.2.3. Miniature Garden Experiment

**A small crop of wheat, corn and bean plants was planted the first night at Alta Floresta and the plants were raised for 8 days following emergence. Photosynthetic radiation was automatically measured at 24-second intervals by a calibrated Apogee PAR detector. The maximum height of the plants (corn and wheat) or the maximum width of their leaves (beans) was measured twice each day (0730 and 1800). Figure 23 summarizes the growth each day and night for the wheat and corn along with the daily photosynthetic flux.**

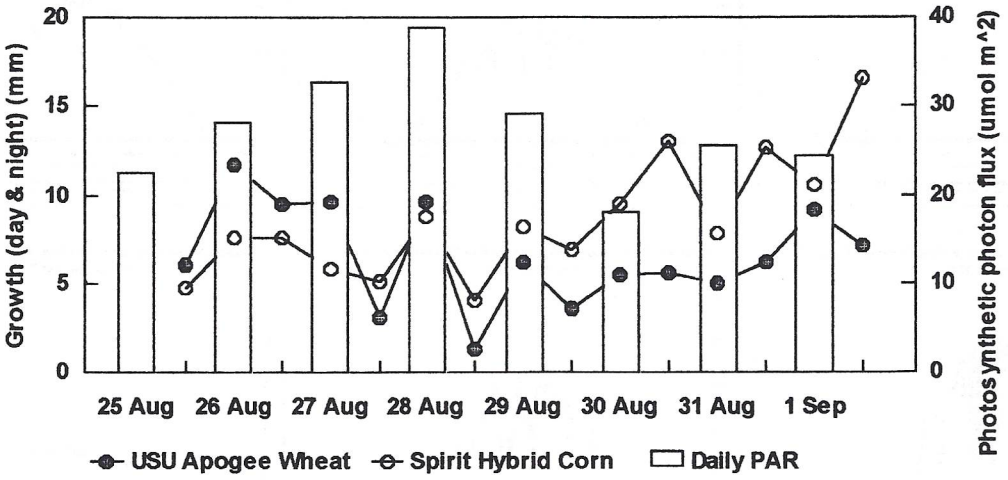


**Fig. 23. Daily growth of wheat and corn and total daily photosynthetic flux.**

**Experimental Method: Eighteen seeds each of corn (Spirit Hybrid), wheat (Utah State University Apogee), beans (Derby bush) and lettuce (Grand Rapids) were planted in commercial potting soil (Jiffy-Mix, Stock No. 6100, Jiffy Products of America, Batavia, Illinois, USA) in a plastic tray having 72 receptacles (Easy Grow Greenhouse, Stock No. 2270, Jiffy Products of America, Batavia, Illinois, USA). After 3 days, the corn and wheat began to emerge as seedlings, and the tray was placed on a roof in full sun for the next 8 days. The plants were watered when the soil became dry to the touch (twice during the 8-day growth period). PAR was measured at 24-second intervals by a PAR detector calibrated by the manufacturer (Apogee Instruments) and temperature of the plastic tray was measured at 24-second intervals by a data logger (Onset). Various other relevant solar irradiance measurements were conducted nearby (e.g. irradiance at 376 nm, which participates in photosynthesis and the phototropic response of plants, and 680 nm, which is near the red peak for photosynthesis). The maximum height of the wheat and corn plants and the maximum width of the leaves of the bean plants were measured twice each day (07:30 and 18:00). As only 1 lettuce seedling emerged, the lettuce were ignored. The data for the bean plants have not yet been processed.**

## 3.2.3. Miniature Garden Experiment

**A small crop of wheat, corn and bean plants was planted the first night at *Alta Floresta and the plants were raised for 8 days following emergence.* Photosynthetic radiation was automatically measured at 24-second intervals by a calibrated Apogee PAR detector. The maximum height of the plants (corn and wheat) or the maximum width of their leaves (beans) was measured twice each day (0730 and 1800). Figure 23 summarizes the growth each day and night for the wheat and corn along with the daily photosynthetic flux.**

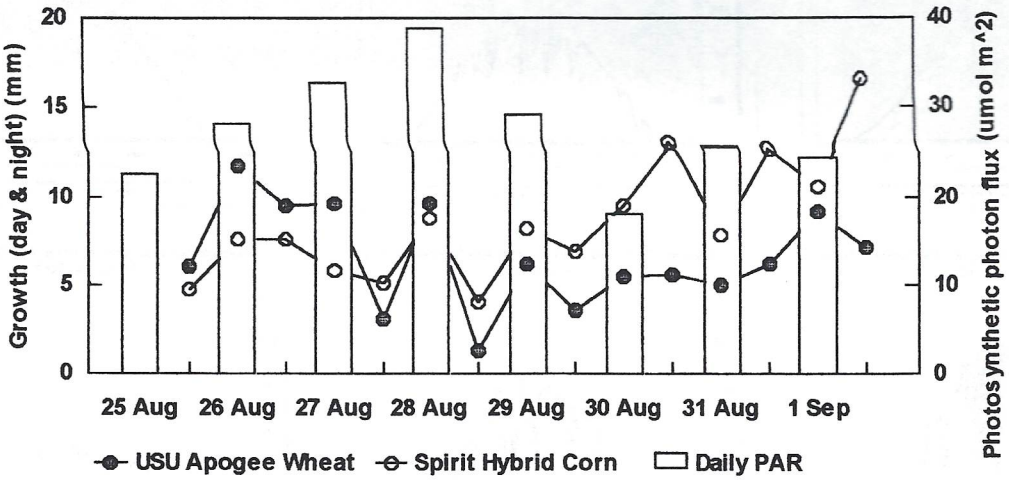


**Fig. 23. Daily growth of wheat and corn and total daily photosynthetic flux.**

**Experimental Method: Eighteen seeds each of corn (Spirit Hybrid), wheat (Utah State University Apogee), beans (Derby bush) and lettuce (Grand Rapids) were planted in commercial potting soil (Jiffy-Mix, Stock No. 6100, Jiffy Products of America, Batavia, Illinois, USA) in a plastic tray having 72 receptacles (Easy Grow Greenhouse, Stock No. 2270, Jiffy Products of America, Batavia, Illinois, USA). After 3 days, the corn and wheat began to emerge as seedlings, and the tray was placed on a roof in full sun for the next 8 days. The plants were watered when the soil became dry to the touch (twice during the 8-day growth period). PAR was measured at 24-second intervals by a PAR detector calibrated by the manufacturer (Apogee Instruments) and temperature of the plastic tray was measured at 24-second intervals by a data logger (Onset). Various other relevant solar irradiance measurements were conducted nearby (e.g. irradiance at 376 nm, which participates in photosynthesis and the phototropic response of plants, and 680 nm, which is near the red peak for photosynthesis). The maximum height of the wheat and corn plants and the maximum width of the leaves of the bean plants were measured twice each day (07:30 and 18:00). As only 1 lettuce seedling emerged, the lettuce were ignored. The data for the bean plants have not yet been processed.**

<----------North----------South---------->

| | | | | | |
|---|---|---|---|---|---|
| Wheat | Wheat | Wheat | Wheat | Wheat | Wheat |
| Wheat | Wheat | Wheat | Wheat | Wheat | Wheat |
| Wheat | Wheat | Wheat | Wheat | Wheat | Wheat |
| Corn | Corn | Corn | Corn | Corn | Corn |
| Corn | Corn | Corn | Corn | Corn | Corn |
| Corn | Corn | Corn | Corn | Corn | Corn |
| Bean | Bean | Bean | Bean | Bean | Bean |
| Bean | Bean | Bean | Bean | Bean | Bean |
| Bean | Bean | Bean | Bean | Bean | Bean |

**Table 2. Organization of miniature garden (lettuce plants were east of wheat section and are not shown as only 3 sprouted).**

## 3.2.4. Results of Miniature Garden Experiment

**Figures 24 and 25 show the growth of all the wheat and corn for 8 days following emergence. Also plotted is the total photosynthetic photon flux for each day. Some of the variation in growth can be attributed to shading by adjacent plants in the miniature garden. As discussed below, other variations are related to reduced sunlight on days with severe aerosol loading.**

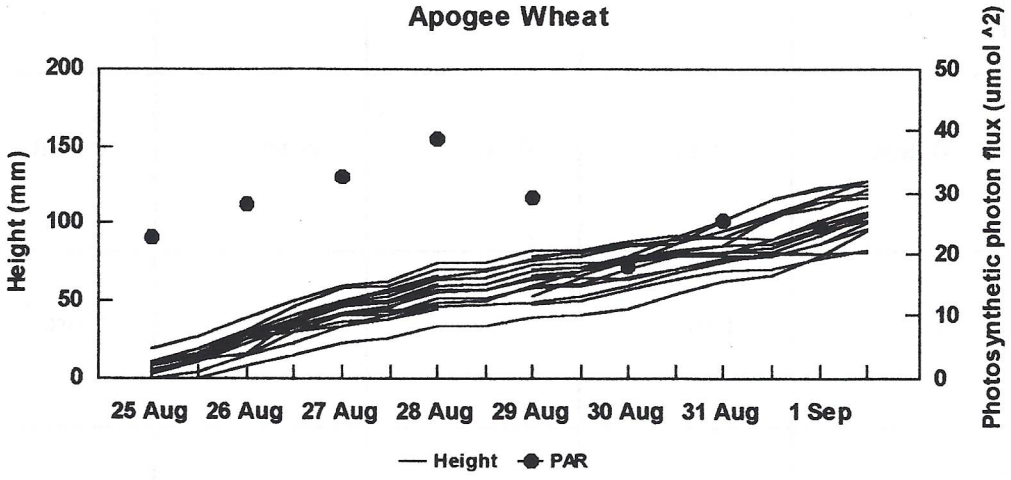


**Fig. 24. Daily height of Apogee Wheat and total photosynthetic flux.**

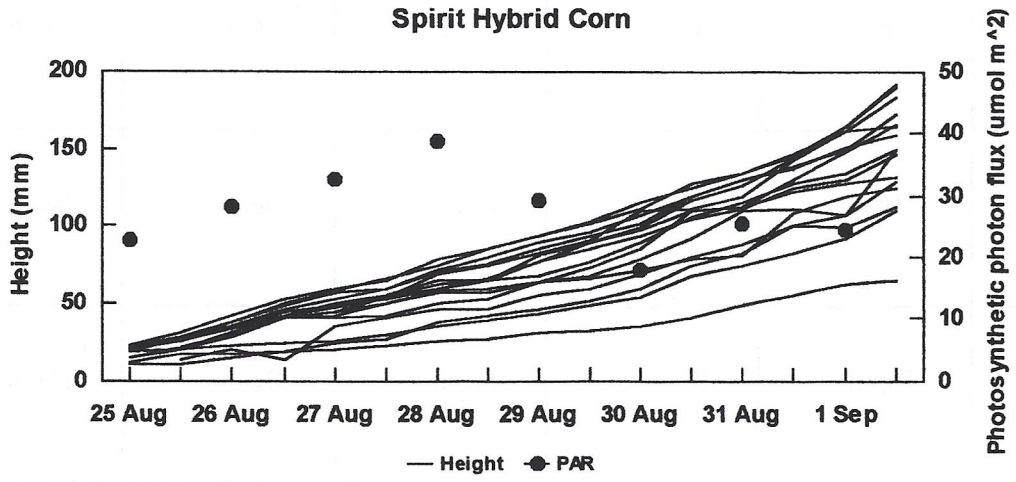


**Fig. 25. Daily height of Spirit Hybrid Corn and total photosynthetic flux.**

It is well established that stem and leaf elongation in plants is greater when PAR is reduced. This mechanism permits stems and leaves to grow into areas with more sunlight. Analysis of the daytime growth of the wheat and corn plants grown at Alta Floresta shows that leaf elongation is inversely related to the total photosynthetic flux (Figs. 26-27). This result confirms that reduced PAR caused by severe aerosol loading can cause leaf elongation, a typical indication of a leaf grown in shade. Other effects of suppressed PAR in plant leaves include thinner epidermal cells and a reduced ratio of the leaf mesophyl to the total leaf area. These effects can cause leaves grown in shade to be poorly adapted to bright sunlight conditions. Thus plants grown during the burning season may be somewhat less prepared for the very high level of PAR which occur after burning season than plants grown under more normal levels of sunlight.

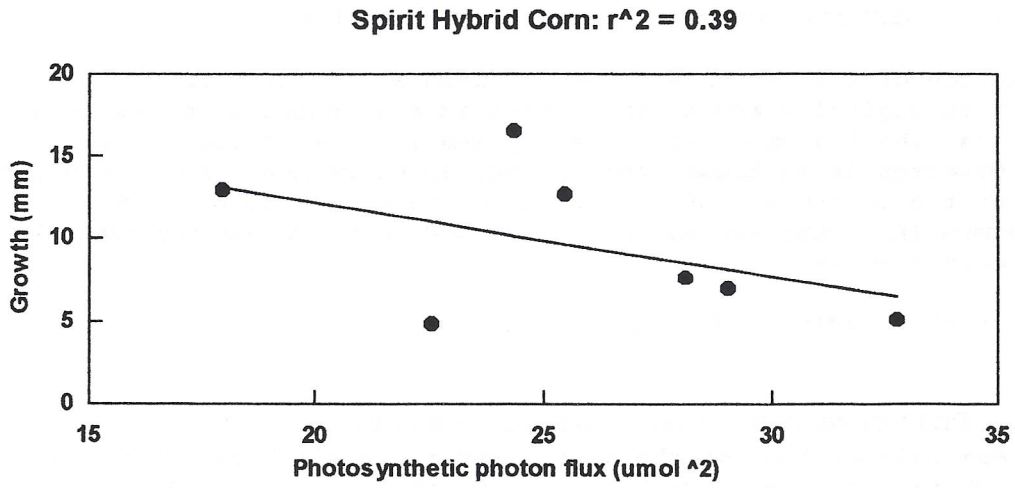


Fig. 26. Scatter graph of the daytime growth of the corn plants and the total photosynthetic photon flux.

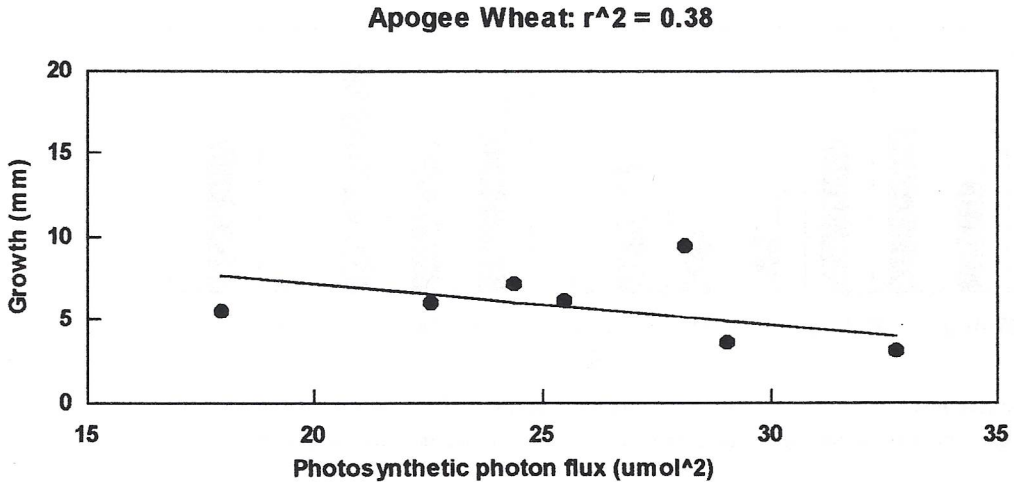


Fig. 27. Scatter graph of the daytime growth of the wheat plants and the total photosynthetic photon flux.

## 3.3. Polarization of the Twilight Sky

Skylight is polarized, with the maximum polarization being 90 degrees from the Sun. When the twilight zenith sky is viewed through an analyzer (e.g. polarized sunglasses or a camera with a polarizer), the zone of maximum polarization appears as a dark band extending to the north and south horizons. Certain birds, fish and insects use polarized skylight as a navigational aid.

Aerosols depolarize skylight. This was readily apparent at Alta Floresta since the zone of maximum polarization was either very subdued or invisible when the zenith sky was viewed through polarized sunglasses at twilight.

### 3.3.1. Sky Polarization Measurement Methodology

The polarization of the zenith sky was measured at sunset using a radiometer with digital readout. The detectors are housed in brass tubes with analyzers. The 520 nm detector is a green light-emitting diode, and the 880 nm detector is an AlGaAs photodiode. In operation, the radiometer is pointed at the zenith sunset, the detector tubes are rotated manually, and the minimum ($P_{max}$) and maximum ($P_{min}$) skylight signals are recorded. The percent polarization is:

$$P(\%) = 100(P_{min} - P_{max})/(P_{min} + P_{max}) \qquad 3\text{-}1$$

### 3.3.2. Sky Polarization Measurement Results

The percentage polarization of the zenith sky at or slightly before sunset for green (520 nm) and near-infrared (880 nm) skylight is shown in Fig. 28.

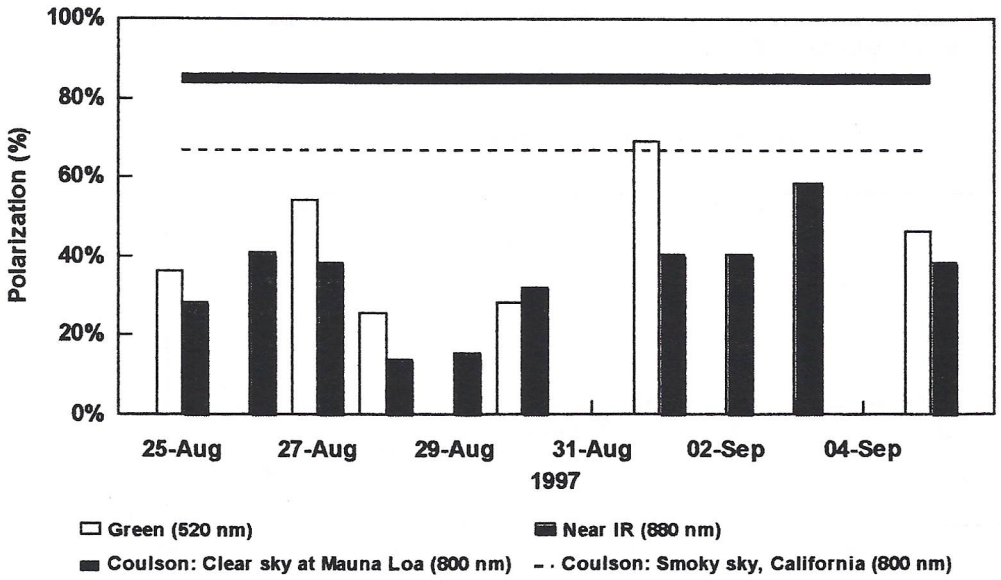


Fig. 28. Polarization of the zenith sky at sunset at Alta Floresta. Measurements by Coulson (1988) of clear sky at MLO and through smoke in California are shown for comparison.

There are few reports in the literature about the depolarization of skylight caused by smoke. A report by Coulson (1988) describes depolarization at 400 and 800 nm caused by smoke from agricultural fires near Davis, California, in 1974. The passage of smoke plumes across the sky is readily apparent in a plot of the degree of polarization versus the zenith angle (Fig. 5.21). The depolarization was much more significant at 400 nm than at 800 nm. Figure 28 shows that the depolarization observed by Coulson was much less than that measured at Alta Floresta.

Certain night-flying migratory birds use the polarization zone as a navigational aid (Able & Able, 1995). Mims (unpublished) has observed grackles and starlings flying parallel to the polarization plane at and after sunset while flying to their roosting sites in South Texas. Mims (unpublished) has also observed southward migrating snow geese in Alaska flying parallel to the zone of polarization at sunset. The prospect that depolarized skylight might affect the habits of certain birds in Brazil during the burning season warrants study.

Polarized skylight is also a navigational cue for various fish and insects. Of particular interest is the reliance of certain bees and ants on polarized skylight. The 1997 fires in Indonesia and Malaysia caused very significant darkening of the sky. Visibility in some locations was reduced to tens of meters, and automobile drivers used headlights during the day. An Internet news item suggested there was concern that bees might not be able to perform their normal pollination function under such conditions. The same might hold for any region of biomass burning where severe aerosol loading causes significant depolarization of skylight. As certain flowering plants and trees were observed to be blooming during the burning season at Alta Floresta, this prospect warrants further study.

## 3.4. Preliminary Tree Ring Study

Reduced photosynthetic radiation and increased amounts of combustion gases in the ambient air can affect the growth of plants, including trees. An Internet query posted prior to this work received various responses pointing out that tropical trees often lack annual growth rings. Could prolonged smoke events produce rings in such trees? Would the width of growth rings in trees with rings be reduced by reduced photosynthetic radiation for 2-3 months each year?

### 3.4.1. Tree Ring Study Methodology

Several living and recently cut and burnt trees were cored. Also, sawn trees and stumps were inspected for the presence of growth rings. Approximately half the sawn trees had evidence of growth rings, although some were difficult to see. Coring trees was quite difficult due to the hardness of the wood.

### 3.4.2. Results of Preliminary Tree Ring Study

The only conclusion that can be drawn from the preliminary tree ring study is that an expanded study is both feasible and reasonable. Measurements of the rings of 3 trees are presented here. It is assumed that the trees described here have a single annual growth ring.

Figure 29 is a plot of the width of the annual growth rings of a large tree which was cut along the Cristalino River ca. 1990. A period of reduced growth approximately matches the onset of deforestation in the Alta Floresta area.

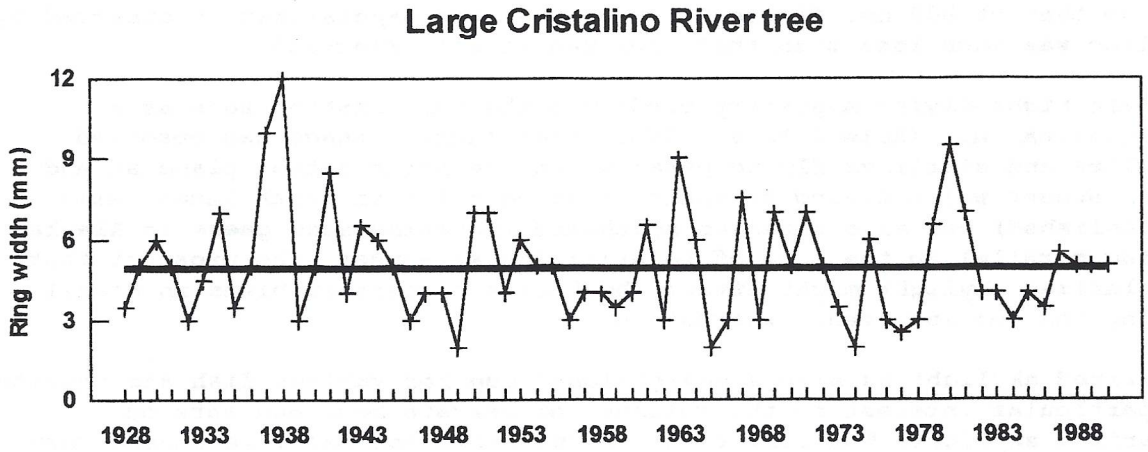


Fig. 29. Width of annual growth rings of a large tree cut near the Cristalino River in ca. 1990. The straight line is the mean width of all the rings.

Figure 30 is a plot of the width of the annual growth rings of a small tree which was cut along the Cristalino River ca.1992. This tree began growing shortly after Alta Floresta began to be settled. Also plotted are the width of the corresponding rings from the much large tree in Fig. 29 above. A cursory comparison of these superimposed plots reveals both similarities and differences between the two trees.

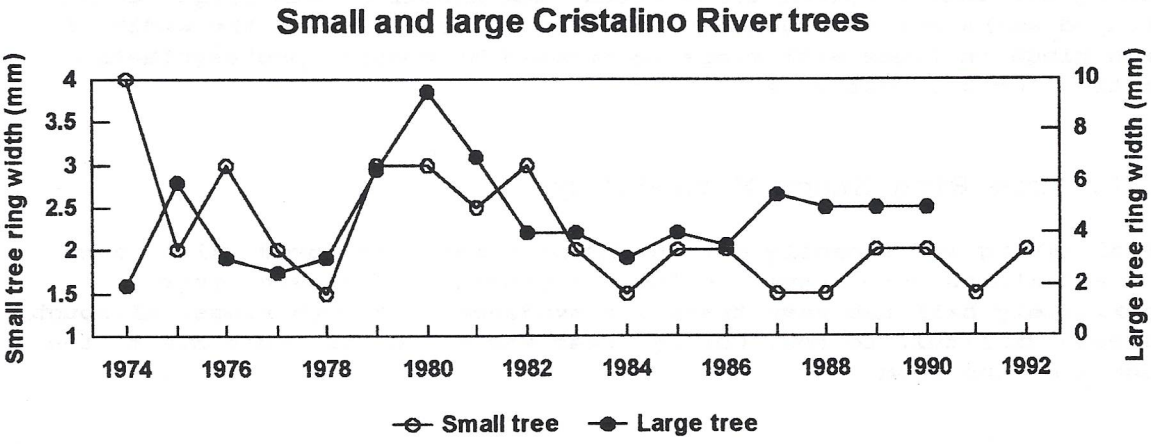


Fig. 30. Width of annual growth rings of a small tree cut near the Cristalino River in ca. 1992. Also plotted are the width of rings from the tree The straight line is the mean width of all the rings.

Figure 31 is a plot of the width of the annual growth rings of a very large, mature *Hymenea algoroba* in Alta Floresta. Only the 13 most recent growth rings are plotted due to the difficulty of coring this tree. Also plotted is the peak aerosol mass concentration measured at Alta Floresta by Artaxo *et al.* (1997). The rings of this tree do not seem to be suppressed as much as those from the trees on the Cristalino River. One possible explanation is that the Cristalino River trees might have a more consistent source of ground water.

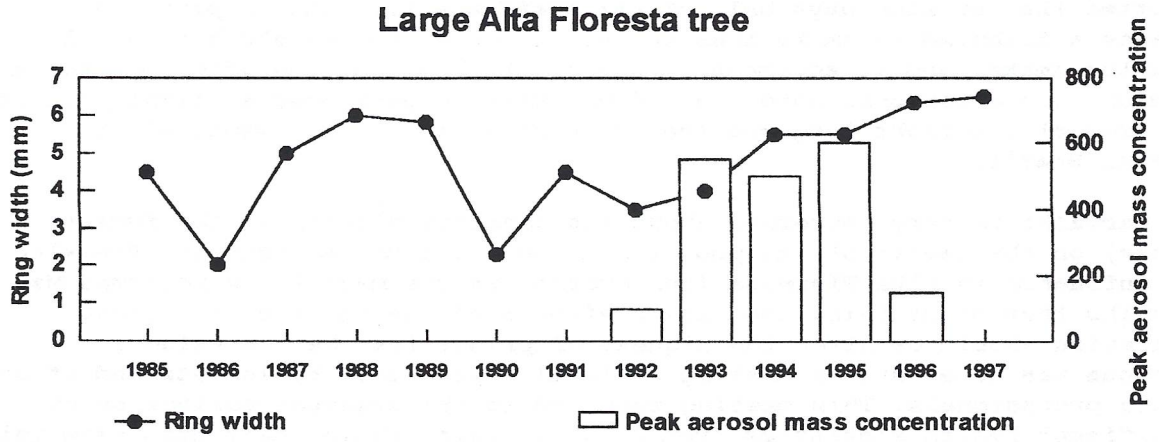


Fig. 31. Width of annual growth rings of a large, mature *Hymaneae algorroba* in Alta Floresta. Also plotted is the peak aerosol mass concentration measured at Alta Floresta by Artaxo *et al.* (1997).are the width of rings from the tree The straight line is the mean width of all the rings.

# 4. EFFECTS OF SMOKE ON THE LOCAL POPULATION

The presence of significant smoke at Alta Floresta had obvious effects on the local population. The odor of smoke was frequently noticeable, especially in early morning when the total column optical depth was lowest but when smoke tends to sink toward the surface and after the olfactory sense has been heightened by the presence of relatively clean, indoor air during the night.

Vitoria Da Riva Carvalho of Floresta Amazonica Hotel e Turisom Ltda. reported that on some days half of her staff was ill with respiratory disease attributed to smoke inhalation. Ms. Carvalho herself became ill from the smoke, and we accompanied her to the hospital one afternoon for a checkup. (On a personal note, one of us (Mims) experienced a slight pain in the area of the right lung and the taste of smoke for 2-3 weeks after leaving Brazil.)

Ms. Carvalho is very concerned about the negative effects of the *fumaca* (smoke) on the health of the population and her tourism business. She also has influence in Alta Floresta (her brother is the mayor). We informed Ms. Carvalho that quantifying the health effects of the smoke on the local population should be given the highest of priorities. Ms. Carvalho's response was to arrange a meeting of local physicians, biologists and other health profssionals. This meeting resulted in the eventual collection of significant health statistics from Alta Floresta. While these data have yet to be fully evaluated, they may represent the most important outcome of our work at Alta Floresta.

## 4.1. Seminar for Health Professionals at Alta Floresta

The purpose of the seminar was to discuss the effects of smoke on the health of the local population. The seminar was opened by Ms. Carvalho, who introduced all those present. A presentation of our research at Alta Flortesta was then given by Mims. The presentation and subsequent discussion were translated by Dr. Ruth Yanagi, a physician from Chicago who is a native of Brazil. Dr. Yanagi and her husband, Dr. R. J. Leider, were in Alta Floresta to join a bird watching excursion to the Cristalino River.

The presentation by Mims was entitled "Possible Ecological Effects of Smoke from Burning of Forests." The topics discussed included (in order):

1. Possible reduced growth of certain crops due to reduced photosynthetic radiation.

2. Possible effects on the growth of trees.

3. Possible reduced growth of algae in the Pantanal and elsewhere.

4. Possible reduced transpiration of trees, which may have implications for river flow.

5. Reduced solar ultraviolet radiation may permit the survival of pathogenic organisms.

6. Respiratory illness caused by particulates and ozone.

7. Reduced diurnal temperature excursions.

8. Reduced polarization of the twilight sky may have an effect on the navigational ability of certain birds.

9. Darkened skies may enhance the number of available breeding sites for photophobic mosquitoes such as *Aedes aegyptii*, which can transmit yellow fever and dengue fever.

Various instruments and experiments-in-progress (bacteria trays and miniature greenhouse) were displayed during the presentation, and various questions were answered. There was then an open discussion about the effects of smoke on the population of Alta Floresta.

The consensus of the health professionals was that half the population of Alta Floresta was then suffering respiratory illness. Dr. Antonio Sinkos stated that prior to this year's burning season he saw 2-3 patients a week with respiratory illness, and that he is now seeing 8 each day. Several physicians expressed concern about their patients who have asthma. Dr. Mario Nishikawa, who manages the Hospital Geral Alta Floresta, expressed serious interest in beginning a formal study of the effects of the burning season on the health of the population. He was especially interested in establishing a protocol for such a study. The most important result of the seminar was that it was agreed to hire a local biology student (for $400) to compile medical records of children ages 0 to 15 and adults over 50 for the past two dry seasons (1996-97).

Seminar attendees included:

Vitoria Da Riva Carvalho (Av. Perimetral Oeste 2001, Alta Floresta, MT CEP 78580-000, Brazil)

R. J. Leider, M.D. (122 S. Michigan Ave., Room 1319, Chicago, Illinois USA)

Ruth Yanagi, M.D. (122 S. Michigan Ave., Room 1317A, Chicago, Illinois USA)

Mario Nishikawa, M.D. (Rua H-1, No. 135, Hospital Geral, Alta Floresta, MT CEP 78580-000, Brazil)

Jose Da Silva Satuinirro, Sanitarista (Rua E4, No. 447, Sec. Mun. Saride, Alta Floresta, MT CEP 78580-000, Brazil)

Antonio Sinkos, M.D. (Rua __, Alta Floresta, MT CEP 78580-000, Brazil)

J. F. Valpassos, M.D. (Av. Aeroporto 7SG/31, Alta Floresta, MT CEP 78580-000, Brazil)

Charles Medeiros, M.D. (Caixo Postal 156, Rua Fum, 118, Alta Floresta, MT CEP 78580-000, Brazil)

Sueide Godoi, M.D. (UNEMAT, CX. P. 324, Alta Floresta, MT CEP 78580-000, Brazil)

Vania Nishioka, M.D., (Rua Ey, 421, Alta Floresta, MT CEP 78580-000, Brazil)

Neusa Maria O. A. Saraion (R: Peixoto Gomde No. 1186, Apto. 123, Sao Paulo, SP, Brazil)

**Edson De Carvalho (Av. Perimetral Oeste 2001, Alta Floresta, MT CEP 78580-000, Brazil)**

**Bradley S. White (280 S. King Street, Seguin, Texas 78155 USA)**

**Forrest M. Mims III (SPAN 433 Twin Oak Road, Seguin, Texas 78155 USA)**

## 4.2. Preliminary Results of the Health Survey

**A very preliminary review of the health statistics compiled by Gisle Cristina de Castro shows several health effects that may be associated with the severe aerosol loading during the burning seasons of 1996 and 1997. Figure xx, for example, shows an increase in recorded deaths during the 1996 burning season and a rise in deaths during the onset of the 1997 burning season.**

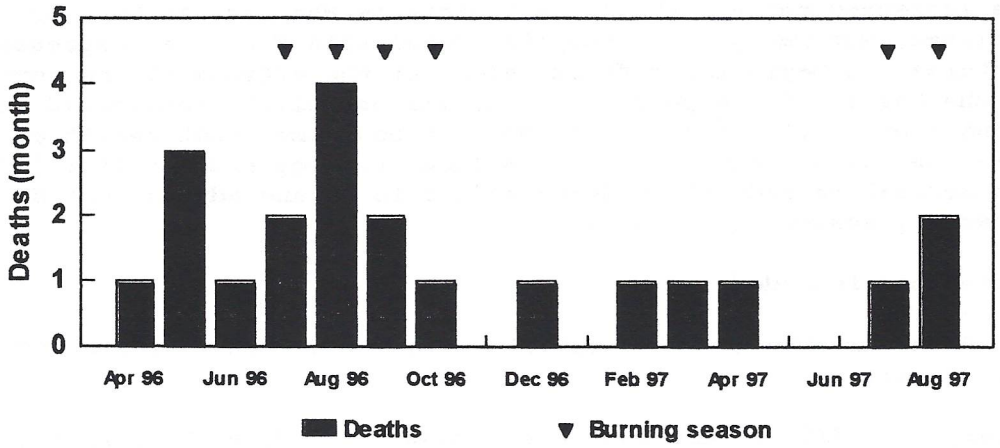


**Fig. 32. Hospital deaths at Alta Floresta (from health statistics compiled by Gisle Cristina de Castro).**

**The incidences of several respiratory diseases at Alta Floresta appear to be positively correlated with the optical depth and negatively correlated with the total UV-B flux. Mims (unpublished) has studied the seasonal association of influenza (type A and B) with diminished UV-B in Houston, Texas, and France. The health statistics at Alta Floresta include statistics for gripe or influenza. (Gripe may also refer to influenza-like diseases.)**

**Figure 33 shows that the normal seasonal peak of influenza near the 1997 winter solstice (21 June) was followed by a second peak in UV-B during the burning season. The second peak, which is longer in duration than the first peak, may or may not be related to the burning season. Viruses are susceptible to UV-B, and the burning season was accompanied by abnormally low levels of UV-B.**

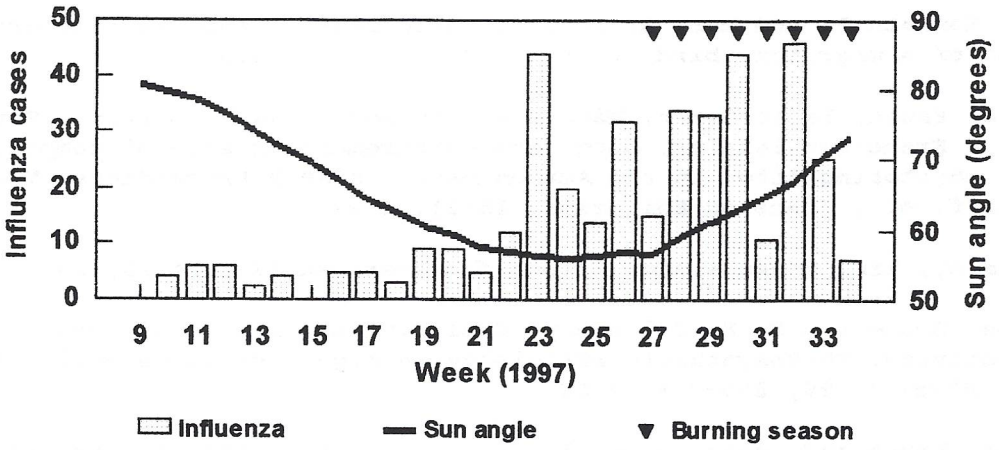


Fig. 33. Influenza cases per week at Alta Floresta. Note the peak near the lowest Sun angle (winter solstice) and the more sustained peak during the burning season.

Figure 34 lends support to the admittedly provocative hypothesis that sharply reduced UV-B during the burning season in Alta Floresta might have contributed to the incidence of influenza. Influenza statistics are available for some days during which UV-B was measured at Alta Floresta. Influenza has an incubation of 1 to 5 days and causes the most discomfort and fever for 2-5 days fever. The influenza cases in Fig. 34 have been lagged by 5 days to account for the average of these incubation and fever times. The resulting correlation ($r^2$) of daily influenza cases and the daily UV-B flux is 0.82.

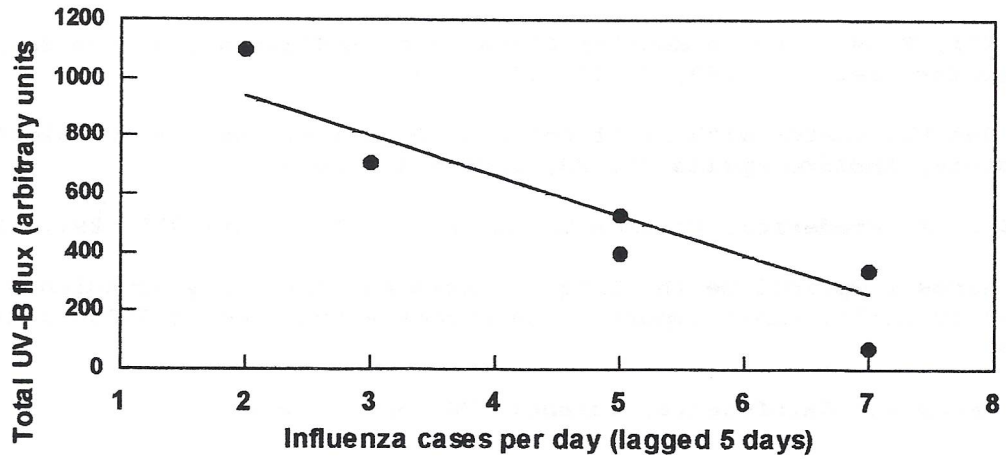


Fig. 34. This scatter graph shows a high correlation ($r^2$ = 0.82) of daily influenza cases and total UV-B flux at Alta Floresta.

## REFERENCES

Able, Kenneth P. and Mary A. Able, Interactions in the flexible orientation system of a migratory bird, *Nature* 375, 230-232, 1995.

Artaxo, Paulo, Fábio Gerab, Márcia A. Yamasoe, José V. Martins, Karla M. Longo & Francisco Echalar, Long term measurement of aerosol composition at three monitoring sites in the Amazon basin, SCAR-B Proceedings, V.W.J.H. Kirchoff, ed., Transtec Editorial, 15-21, 1997.

Beardsley, Tim, Smoke alarm, *Scientific American* 277, 24-25, 1997.

Bugbee, Bruce and F. B. Salisbury, Exploring the limits of crop productivity: Photosynthetic efficiency in high irradiance environments, *Plant Physiol.* 88, 869-878, 1988.

Bugbee, Bruce and Oscar Monje, The limits of crop productivity, *BioScience* 42, 494-502, 1992.

Galindo, I., S. Frenk. and H. Bravo, Ultraviolet irradiance over Mexico City, *J. of the Air & Waste Management Association* 45, 886-892, 1995.

Herman, J. R., P. K. Bhartia, O. Torres, C. Hsu, C. Seftor and E. Celarier, Global distribution of UV-absorbing aerosols from Nimbus 7/TOMS data, *J. Geophy. Res.* 102, 16,911-16922, 1997.

Holben, B. N., A. Setzer, T. F. Eck, A. Pereira and I. Slutsker, Effect of dry-season biomass burning on Amazon basin aerosol concentrations and optical properties, *J. of Geophys. Res.* 101, 19,465-19,482, 1996.

Krueger, A. J., Sighting of El Chichón sulfur dioxide clouds with the Nimbus 7 Total Ozone mapping Spectrometer, *Science* 220, 1377-1378, 1983.

Lewan, Todd, Study: Amazon forest is a tinderbox, Associated Press, 3 December 1997

Mims III, F. M., How to Monitor Ultraviolet Radiation from the Sun, *Scientific American*, 263, 2, 106-109, 1990.

---, Sun Photometer with Light-Emitting Diodes as Spectrally Selective Detectors, *Applied Optics* 31, 33, 6965-6967, 1992.

--- & J. E. Frederick, Cumulus Clouds and UV-B, *Nature* 371, 291, 1994.

---, Aerosol Optical Depth, Ultraviolet-B and Total Sky Irradiance during SCAR-B (Brazil), final report, NASA purchase order No. S-59036-Z/GSFC, 1995a.

---, Smoke and Rainforests, *Science* 270, 5243, 1995b.

---, Significant Reduction in UV-B Caused by Smoke from Biomass Burning in Brazil, *Photochemistry and Photobiology*, 64, 123-125, 1996a.

---, UV Radiation and Field Experiments, *BioScience* 46, 564-565, 1996b.

---, Significant reduction of UVB caused by smoke from biomass burning in Brazil, *Photochem. and Photobio.* 64, 814-816, 1996c.

---, Biological Effects of Diminished UV and Visible Sunlight Caused by Severe Air Pollution, *IRS '96: Current Problems in Atmospheric Radiation, Proceedings of the International Radiation Symposium*, A. Deepak Publishing, 905-908, 1997a.

---, Brent N. Holben, Thomas F. Eck, Brian C. Montgomery and William B. Grant, Smoky Skies, mosquitoes, and disease (letter), *Science* 276, 1774-1775, 1997b.

---, Health effects of tropical smoke (letter), *Nature* 390, 222-223, 1997c.

Yanhong, Tang, Kachi Naoki, Furukawa Akio & Muhamad Awang, Light reduction by regional haze and its effect on simulated leaf photosynthesis in a tropical forest of Malaysia, *Forest Ecology and Management* 89, 205-211, 1996.

Tong, Yongyi and Bruce Lighthart, Solar radiation is shown to select for pigmented bacteria in the ambient outdoor atmosphere, *Photochemistry and Photobiology* 65, 103-106, 1997.

# Appendices



Portions of Appendices 2-5 are adapted from Mims, F. M., Aerosol Optical Thickness, Total Ozone, UV-B, Diffuse/Total Solar Irradiance and Sky Polarization Through Forest Fire Smoke and Stratospheric Aerosols During TOMS Overpasses, Report to GSFC (Purchase Order No. S-78417-Z), 30 Dec 1996.

## Appendix 1. Correspondence in *Science* and *Nature* regarding infectious disease and severe aerosol loading

This work was immediately preceded and followed by letters published in *Science* and *Nature*. These letters are reproduced here as they discuss the possible association of infectious disease and sharply reduced solar UV-B caused by severe aerosol loading.

# Appendices

1. Correspondence in *Science* and *Nature* regarding infectious disease and severe aerosol loading

2. Instrumentation

3. Sun Photometer Calibration

4. Ozonometer Calibration

5. Measurement Errors

Portions of Appendices 2-5 are adapted from Mims, F. M., Aerosol Optical Thickness, Total Ozone, UV-B, Diffuse/Total Solar Irradiance and Sky Polarization Through Forest Fire Smoke and Stratospheric Aerosols During TOMS Overpasses, Report to GSFC (Purchase Order No. S-78417-Z), 30 Dec 1996.

## Appendix 1. Correspondence in *Science* and *Nature* regarding infectious disease and severe aerosol loading

This work was immediately preceded and followed by letters published in *Science* and *Nature*. These letters are reproduced here as they discuss the possible association of infectious disease and sharply reduced solar UV-B caused by severe aerosol loading.

pp. 1774-5
ISSN 0036-8075
20 JUNE 1997
VOLUME 276
NUMBER 5320

SCIENCE

AMERICAN ASSOCIATION FOR T ADVANCEMENT OF SCIENCE

# LETTERS

## Smoky Skies, Mosquitoes, and Disease

The report "Direct radiative forcing by smoke from biomass burning" by Peter V. Hobbs *et al.* (21 Mar., p. 1776) discusses the regional nature of a massive aerosol source in Brazil and suggests a possible effect on global climate. A more immediate concern is respiratory disease associated with particulate inhalation (*1*). Additional concerns are regional scale reductions in photosynthesis and the possibility of increased incidence of infectious and mosquito-transmitted disease.

In regions of intensive biomass burning in the tropics, the Amazon in particular, the photosynthetically active spectrum of sunlight (wavelengths of 400 to 700 nanometers) is reduced approximately 35 to 40% for 2 months (*2*). Ultraviolet-B (UV-B) in natural sunlight kills airborne bacteria (*3*), and exposing drinking water to normal intensities of UV-B has reduced diarrhea in children in Kenya by 33% (*4*). Thus, the sharply diminished (by more than 80%) UV-B during the burning season in Brazil (*5*) might enhance the populations of infectious pathogens suspended in air and water.

There is an increasing incidence of yellow fever in Brazil, Bolivia, and sub-Sahara Africa (*6*). The larvae and pupae of some disease-transmitting mosquitoes (including *Aedes aegypti*, an important vector for yellow fever and dengue fever, and *Culex pipiens*, which can transmit encephalitis) are highly photophobic to the UV-A and green wavelengths of sunlight. During the 1995 burning season in Brazil, regional smoke reduced sunlight in the UV-A (340 nanometer wavelength) range as much as 74% and in the green (500-nanometer wavelength) range as much as 45% near Cuiabá, far from the region of maximum burning (*5*). Experiments with wild populations of *C. pipiens* show that, when given a choice of nursery sites with eight gradations of natural illumination, females deposit their eggs in the darkest nurseries (*7*), and their larvae avoid UV (*8*).

The possibility that severe aerosol loading in the tropics can cause respiratory disease, suppress photosynthesis, increase the number of darkened mosquito nurseries, and enhance the survival of pathogenic microorganisms suspended in air and water warrants investigation. Such investigation might also shed light on other biological effects of severe aerosol loading.

**Forrest M. Mims III**
*Sun Photometer Atmospheric Network,*
*433 Twin Oak Road,*
*Sequin, TX 78155, USA*
*E-mail: fmims@aol.com*
**Brent N. Holben**
**Thomas F. Eck**
*Biospheric Sciences Branch,*
*Goddard Space Flight Center,*
*National Aeronautics and Space Administration (NASA),*
*Greenbelt, MD 20771, USA*
*E-mail: brent@spamer.gsfc.nasa.gov*
*E-mail: tom@spamer.gsfc.nasa.gov*
**Brian C. Montgomery**
*Uniformed Services University of the Health Sciences,*
*Goddard Space Flight Center, NASA*
*E-mail: brianm@nullspace.gsfc.nasa.gov*
**William B. Grant**
*Langley Research Center, NASA*
*Hampton, VA 23681–0001, USA*
*E-mail: w.b.grant@larc.nasa.gov*

### References

1. D. J. Schemo, *New York Times*, 13 October 1995, p. A3.
2. T. F. Eck, B. N. Holben, I. Slutsker, in *Smoke, Clouds, and Radiation—Brazil, Proceedings*, V. W. J. H. Kirchhoff, Ed. (Transtec, Sao Jose dos Campos, Brazil, 1996, pp. 45–48.
3. N. Munakata *et al.*, *Photochem. Photobiol.* **63**, 74 (1996).
4. R. Conroy, *Lancet* **348**, 1695 (1996).
5. F. M. Mims III, *Photochem. Photobiol.* **64**, 814 (1996).
6. S. E. Robertson *et al.*, *J. Am. Med. Assoc.* **276**, 1157 (1996).
7. F. M. Mims III, *Int. Radiat. Symp.*, in press.
8. ———, *BioScience* **46**, 564 (1996).

Correspondence in *Nature* 390, 222-223, 20 Nov 1997 (copyright by *Nature*):

# Health Effects of Tropical Smoke

Since August large portions of Indonesia and Malaysia have been subjected to prolonged episodes of thick haze caused by smoke from intentionally set fires, primarily in Sumatra and Borneo. As reported in Nature (1,2) and in many Internet web sites (3), the haze has caused a serious health emergency for millions of people and many species of animals and has adversely affected agriculture. A report (4) on the incidence of upper respiratory tract infections (URTI) in Sarawak, Malaysia, shows that the average daily hospital and clinic visits from 5-28 August was 593 per day while the average daily visits for 1996 were 346 per day. A more recent plot of hospital and clinic visits in Sarawak (5) shows a very significant increase in URTI admissions in September, exceeding 3,000 on 23 September. The incidence of URTI was associated with an extraordinarily high air pollution index (API), which exceeded 900 on 23 September. An API >400 is considered life-threatening.

Although deforestation in Africa and South America has received considerably less notice than the Asian crisis, there was considerable smoke over substantial portions of these continents during the 1997 burning season. Satellite observations show that half of Brazil was covered by smoke during parts of August and September. The consensus of a meeting of physicians and health officials in Alta Floresta, Brazil, on 27 August, which was organised to hear results of my ongoing UV-B, optical depth and airborne bacteria studies there, was that half the local population was suffering from respiratory disease. Dr Antonio Sinkos stated that he saw "2-3 patients per week [with respiratory disease] before the burning and now 8 a day." He and his colleagues expressed particular concern about the effects of the smoke on asthmatics, children and the elderly. Health statistics for Alta Floresta are now being compared with measurements of optical depth and UV-B.

Studies of the health effects of severe air pollution in urban areas are complicated by multiple pollutant sources. The importance of the data from Sarawak and Alta Floresta is that they provide important information about the health effects of a single source of pollution, biomass burning. When combined with measurements of sharply diminished UV-B associated with thick smopke, these data also provide an important opportunity to study the increased incidence of disease caused by pathogenic bacteria and viruses which are ordinarily inactivated by solar ultraviolet (6).

Although laws prohibit or regulate biomass burning in Indonesia and Brazil, their enforcement is either lax or difficult. Until enforcement is achieved, there is a real possibility of smoke emergencies in future years. Countries at risk have a responsibility to prepare for future smoke emergencies, perhaps with the assistance of the international community and the UN Department of Humanitarian Affairs (7).

Medical and scientific emergency response teams should be organised for immediate deployment to regions with serious smoke problems. Medical teams should be prepared to distribute suitable respirators (not merely dust masks), medical supplies and tracts that advise people why and how to avoid smoke. Scientific teams should be equipped with portable Sun photometers, radiometers and aerosol collectors. Observers in developing countries with limited budgets can assemble very inexpensive, accurate Sun photmeters from readily available components (8, 9). A few dozen scientists in Brazil, the United States and elsewhere have considerable experience making smoke-related measurements and could participate in an international response to major smoke emergencies. All data should be freely shared among

team members and scientists from the host countries.

The TOMS (Total Ozone Mapping Spectrometer) satellite instrument can reliably detect the presence of smoke over land (10). Optical depth measurements of smoke in biomass burning regions can provide important calibration data for this instrument. The close association of upper respiratory diseases with optical depth in Alta Floresta and the API in Sarawak suggest the possibility of using TOMS as an epidemiological tool to identify regions which might have smoke-related respiratory disease.

Forrest M. Mims III
*Sun Photometer Atmospheric Network,*
*433 Twin Oak Road,*
*Seguin, Texas 78155 USA*
*e-mail: fmims@aol.com*

---

1. Swinbanks, D. *Nature* 389, 321 (1997).

2. *Nature* 389, 315 (1997).

3. http://www.geocities.com/hotsprings/2188/haze.html (1997).

4. Environmental Health Unit, The haze in Sarawak, Epidem. News 7 (1997) available at http://ftp.http://ftp.sarawak.com.my/org/jkns/haze97/haze1.htm (1997).

5. http://ftp.sarawak.com.my/org/jkns/haze97/haze2.htm (1997).

6. Mims, F.M. *et al. Science* 276, 1774-1775 (1997).

7. UN Dept. of Humanitarian Affairs, http://www.reliefweb.int (1997).

8. Carlson, S. *Sci. Amer.* 276, 106-107 (1997).

9. Concord Consortium http://www.concord.org/haze/ (1997).

10. Herman, J.R. *et al. J. Geophys. Res.* 102, 16,911-16922 (1997); http://jwocky.gsfc.nasa.gov/.

# Appendix 2. Instrumentation

Relatively simple instruments, such as Sun photometers and polarimeters, can be used to detect atmospheric aerosols. In the fall of 1988, well before the TOMS aerosol capability was developed, Sun photometer observations were made in South Texas during TOMS overpasses. In September 1988, smoke from the historic Yellowstone forest fires arrived over South Texas. For several days the hue of the cloud-free sky was brownish-yellow. Measurements with a Sun photometer showed significant reductions in direct irradiance at 300 nm (Mims, 1990). On these days TOMS measurements showed slight increases in total ozone which may be related to tropospheric ozone produced as a byproduct of biomass burning.

The 1988 observations of the Yellowstone smoke in Texas contributed to the development of various kinds of miniature Sun photometers, radiometers and other instruments used during this study. Most of these instruments were also used in Brazil in 1995 during a NASA-sponsored segment of SCAR-B in Brazil (Mims, 1995a). These instruments have also been used in field trips and eclipse studies in Japan, Switzerland, Argentina, Chile, Alaska, Hawaii, Mexico, across the United States and during a circumnavigation of North America.

## Appendix 2.1. MicroTOPS-7 Ozonometer and Sun Photometer

MicroTOPS-7 (MTOPS-7) is one of ~30 microprocessor-controlled Sun photometers that almost simultaneously observe the direct Sun (~2° field of view) at 297, 303, 310, 940 and 1020 nm. The instrument stores up to 40 scans of the 5 channels in its non-volatile memory. The data can be downloaded into an external PC via a serial port in real time or at any later time. For this study, the data were downloaded in real time directly into a spreadsheet in a hand-held computer, which provided an immediate calculation of total ozone and optical thickness. Appendix 4 discusses the ozone retrieval method.

MTOPS-7 observes the atmosphere's aerosol optical thickness at the atmospheric window of 1020 nm. The extraterrestrial constant required for these derivations is derived from Langley observations at Mauna Loa Observatory. Calibration of the MTOPS-7 $AOT_{1020nm}$ channel is discussed in Appendix 2. Additional details will be described in a forthcoming publication.

The ratio of 940 and 1020 nm observations by MTOPS-7 is proportional to the column abundance of water vapor in a column through the atmosphere. Preliminary work shows good agreement with expected values of column water vapor (using the well-known correlation of dew point and precipitable water). However, the water vapor calibration of MTOPS-7 is not yet complete and MTOPS-7 results not given here. Instead, Microtops II column water vapor amounts are given. As during SCAR-B, MTOPS-10 served as a backup to MTOPS-7. Since MTOPS-7 worked well, MTOPS-10 was not used.

## Appendix 2.2. SUNTOPS 5-Channel Sun Photometer

SUNTOPS is a MicroTOPS in which spectrally-selective light-emitting diodes (LEDs) replace conventional photodiodes and interference filters (Mims 1992). As with MicroTOPS, SUNTOPS data were downloaded in real time into a spreadsheet in a hand-held computer. This permitted the AOT at the principle wavelengths of interest to be determined immediately. Calibration of SUNTOPS is discussed in Appendix 3.

The peak wavelengths detected by SUNTOPS are 376, 540, 620, 680 and 850 nm. The wavelength of principle interest to this study is 376 nm, which is close to the 380 nm TOMS aerosol channel. This wavelength is sensed by a gallium nitride LED operated as a spectrally-selective photodiode with a full width, half maximum (FWHM) bandpass of 16 nm. (see Mims, 1992). Annual Langley method calibrations at MLO from 1992 to 1996 of a Sun photometer using LEDs as photodetectors yields a coefficient of variation of about 1%, which shows that these detectors are exceptionally stable. The original SUNTOPS, which was used during SCAR-B (Mims 1995b), used interference filters with a peak bandpass of 340, 600, 630, 760 and 780 nm. When the data acquired using SUNTOPS during SCAR-B were being processed, it was found that the 600 nm interference filter had experienced significant drift. To avoid future filter problems, in May 1996 all the interference filters and detectors were removed and replaced by carefully selected, spectrally dependent light-emitting diodes (LEDs). The revised SUNTOPS was then calibrated using the Langley method at Mauna Loa Observatory in 1996 and 1997. Although the bandpass of LEDs operated as photodetectors exceeds that of interference filters (about 12 to 50 nm, FWHM), it is anticipated that these detectors will prove much more stable than conventional detectors and interference filters.

## Appendix 2.3. Microtops II Ozonometer and Sun Photometer

Microtops II is a commercial version of the original MicroTOPS (Morys *et al.*, 1996). The instrument used in this study measures the same 5 wavelengths as MicroTOPS. However, the UV-B filters have a bandpass of only 2.5 nm as opposed to the 7 nm filters used in MicroTOPS. This increases the range of $\mu$ (the ozone mass) over which Microtops II can provide accurate ozone retrievals.

Microtops II incorporates a built-in computer and real time clock which calculates the Sun angle, air mass and $\mu$ for the geographic coordinates keyed in by the user. The coordinates were provided by a Global Positioning Satellite receiver. The instrument also computes the total ozone and water vapor. More than 800 scans of the 5 channels can be stored in the instrument's non-volatile memory. Data can be sent to an external computer over a serial port.

## Appendix 2.4. Erythemal Action Spectrum UV-B Radiometers

The erythemal action spectrum was measured with a miniature phosphor-based detector made and calibrated by the Solar Light Company. The solar UV-B index measured by this detector agrees well with that measured with a Solar Light Model 501 Biometer and Brewer Spectrophotometer No. 112 during a comparison at Seguin, Texas during the summer of 1995.

## Appendix. 2.5. Total-Sky and Diffuse Irradiance Radiometer

The diffuse and total-sky irradiance was measured for the erythemal UV-B and at 308, 340, 376, 500 and 650 nm. UV-B observations were made using the Solar Light erythemal UV-B detectors described above. The remaining wavelengths were measured with miniature probes fitted with Teflon diffusers having good cosine response. The 308, 340 and 500 nm probes use narrow bandpass (7 and 10 nm FWHM, respectively) interference filters and the 376 and 650 nm probes use LEDs as spectrally selective detectors. Diffuse radiation was measured by shading each detector's diffuser with a disk mounted on a thin rod.

A brief, preliminary description of the irradiance probes and data loggers has been published (Mims and Frederick, 1994), and a more complete paper on these instruments is in preparation.

## Appendix 2.6. Polarimeter

The atmosphere efficiently polarizes sunlight. The maximum polarization of a clear sky appears to the observer as an arc 90 degrees away from the Sun. Since scattering from aerosols depolarizes skylight, polarization measurements were made during this study.

The polarization of the sky was measured with a simple polarimeter at or before sunset on most evenings. The polarimeter is a high-gain amplifier (Mims, 1990). Two polarization probes were used. One is a light-emitting diode with a spectral response peaking near 520 nm fitted with an analyzer and installed in a brass collimator. The other is an AlGaAs photodiode with a peak sensitivity of 880 nm fitted with a Polarcor analyzer and installed in a brass collimator. In operation, the probs are pointed at the zone of maximum polarization (e.g. the zenith sky at sunset) and manually rotated. The maximum anbd minimum signals are used to determine the degree of polarization (Eq. 1). The design of the polarimeter is based on informative discussions with and demonstrations by Frederick Volz at his home in Lexington, Massachusetts in 1996.

The polarization (P) is calculated from:

$$P = (I_{max} - I_{min})/(I_{max} + I_{min}) \quad (1)$$

where,

$I_{max}$ is the signal when the analyzer is rotated to yield the maximum signal and

$I_{min}$ is the signal when the analyzer is rotated to yield the minimum signal.

The 520-nm wavelength was selected since this is near the wavelength region of maximum polarization (Coulson, 1975). This wavelength is also near the peak spectral response of insects and, presumably, birds that use polarized skylight for navigation. The 880-nm wavelength was selected since Coulson (1988) and others have shown that near infrared wavelengths greater than 700 nm are much better suited for studying depolarization caused by stratospheric aerosols.

## Appendix 2.7. Cameras and Film

**Two Fuji 28/45 mm Mini/Dual Plus 35 mm cameras were taken to Brazil. One camera was kept loaded with Kodachrome 64 color slide film and the other with Kodacolor 100 color print film.**

**A Pentax Super Program equipped with a 50m lens and extension tube or a 180 degree fisheye lens was used to photograph agar trays and to make all-sky photographs centered at the zenith.**

## Appendix 2.8. Miscellaneous Instruments, Software and Data Sources

**Geographic coordinates were provided by a Global Positioning Satellite receiver (Garmin GPS 38). Temperature, relative humidity and dew point were measured by a miniature hygrometer (Mannix Model LAM880D). Atmospheric pressure was measured by an electronic barometer (Casio). Acquisition and processing of data from MicroTOPS-7 and SUNTOPS was achieved using a pocket computer (Hewlett-Packard HP-100) loaded with a program (Software Wedge, Tal Enterprises) which permits serial data to be entered into a working spreadsheet (As-Easy-As). Instruments with real time clocks were updated using time signals provided by the GPS receiver or time signals broadcast by WWV and received by a miniature shortwave receiver (Sony ICF SW-20).**

**Data analysis and preparation of this report were performed using As-Easy-As (for downloading real time data in the field), Lotus 1-2-3 (vers. 4 and 5), Jandel Scientific TableCurve, CSS Statistica and WordPerfect 6.1. Various Internet sources provided GOES images of cloud cover and hot spots. Color copies of the Kodacolor prints used as plates in this report were made using a Canon 8000 color copier (Kinkos).**

# Appendix 3. Sun Photometer Calibration

This work uses the aerosol optical thickness (AOT) equation based on Beer's Law and derived by Frederick E. Volz (1959). The equation, which is applicable to near-monochromatic light ($AOT_\lambda$) is:

$$AOT_\lambda = [\ln I_o - \ln I - (\tau_R\ m\ p/p_o)]\ m^{-1} \qquad (2)$$

where,

$I_o$ is the extraterrestrial constant at the mean Earth-Sun distance,

I is the measured solar radiation corrected to the mean Earth-Sun distance,

$\tau_R$ is the $AOT_\lambda$ (m = 1) due to Rayleigh scattering at the measured wavelength,

m is the optical air mass corrected for the Earth's curvature, and

$p/p_o$ is the ratio of the measured pressure to the pressure at sea level.

The extraterrestrial constants ($I_o$) for the various Sun photometers used in this study were determined using the Langley method at Mauna Loa Observatory in May 1996 and 1997. During calibration, 5 rapid sequence scans are made at frequent intervals during a complete morning. The scans are not averaged, and all data between a reasonable range of air masses (~1.5 to 5) are used to compute the regression line. In all cases the natural logarithm of the signal was plotted against the air mass. Thus the exponential $AOT_\lambda$ is derived, not the decadic $AOT_\lambda$ which results when the logarithm (base 10) is plotted against the air mass (Fig. A-1).

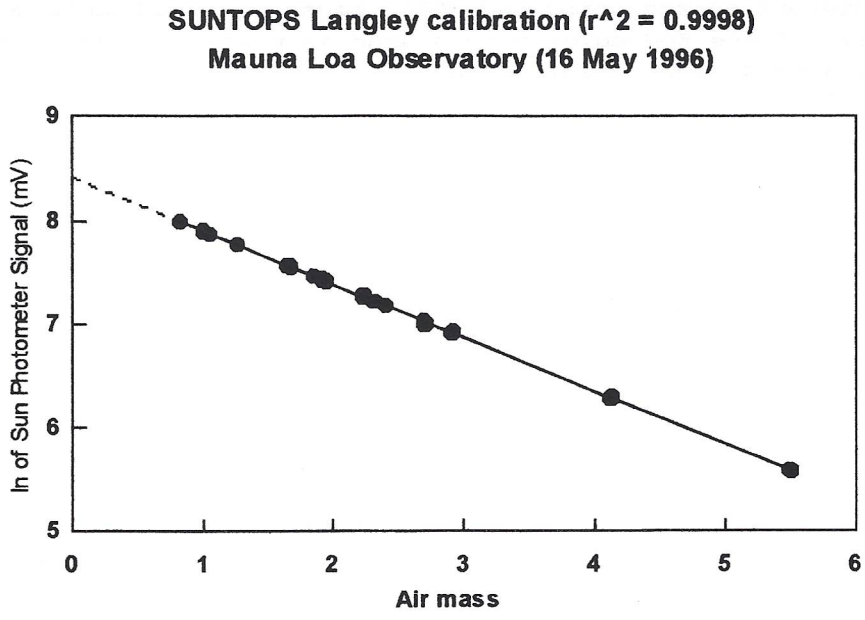


Fig. A-1. Langley-method determination of the extraterrestrial constant, $I_0$ (the intercept at the y axis), of the 376-nm channel of SUNTOPS at Mauna Loa Observatory (16 May 1996). Minimum air mass is <1 due to the low pressure at the altitude of MLO (3.4 km).

It was once common practice to express the extinction caused by aerosols as the transmission (T) of the direct solar beam. Although expressing extinction using T has fallen out of favor, it provides a more intuitive means for expressing extinction, and it was the method used by the Astrophysical Observatory (APO) of the Smithsonian Institution for more than 60 years. Therefore, the tabulated $AOT_\lambda$ data in this report are also presented as transmission coefficient using:

$$T = \exp(-AOT_\lambda) \quad (3)$$

Note that Eq. 2 applies to exponential $AOT_\lambda$. Decadic extinction $AOT_\lambda$, which was used by the APO, is converted to T using:

$$T = \log_{10}(-AOT_\lambda) \quad (4)$$

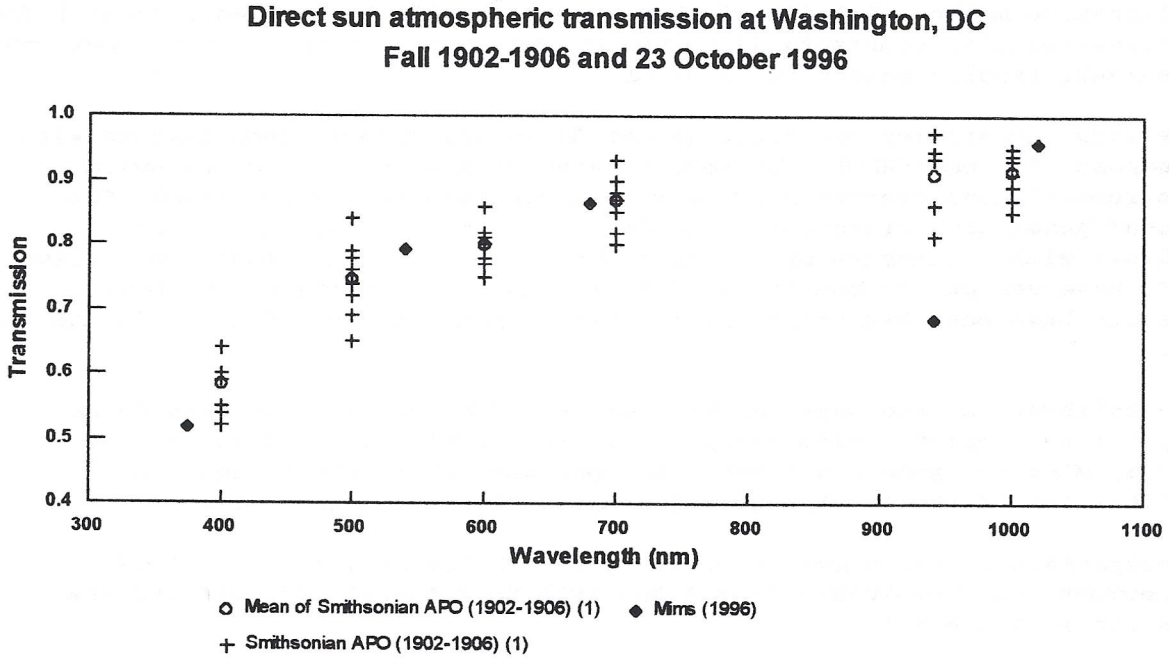


1. Annals of the Astrophysical Observatory of the Smithsonian Institution, Vol. II, 98, Table 14 (1908).

Figure A-2 shows T measured on a relatively clear fall day in Washington, DC, using SUNTOPS and MicroTOPS-7 along with T measured by the APO on clear days in Washington from 1902 to 1906. (The low value of $AOT_{940nm}$ measured by SUNTOPS is due to water vapor.) Note that the data in this plot include transmission loss caused by Rayleigh scattering. All other optical thickness data in this report are for aerosols, the Rayleigh component having been subtracted.

# Appendix 4. Ozonometer Calibration

The original two TOPS instruments (300 and 305 nm filters with FWHM bandpass of 5 nm) were calibrated against the Nimbus-7/TOMS during the fall of 1990. The ratio of observations by TOPS-1 at 300 and 305 nm was adjusted for the air mass and plotted against the TOMS ozone amount. The function representing the best fit through the points was then used to derive the ozone observed by TOPS. This procedure yielded surprisingly good results. Details of the procedure and a time series of the results from Jan 1990 to Jan 1997 will be included in a paper in preparation.

Ozone retrievals from the ozonometers used in this study were calculated using an equation first derived by Gladys Ungar of TERC and refined by Stanley Anderson of Westmont College. This equation, which is adapted from a single-pair version of the standard Dobson ozone equation, incorporates a correction factor based on a comparison with World Standard Dobson Spectrophotometer (I83) at Mauna Loa Observatory (MLO). (NOAA provides I83 data on the condition that no claim will be made that NOAA endorses this calibration method. Details of this agreement will be sent on request.) The extraterrestrial constants ($I_o$) used in the ozone equation are derived from clear-sky Langley observations at MLO.

The first generation MicroTOPS (Rolex Award instrument) uses filters with a bandpass of 7 nm (FWHM). The second generation SuperTOPS (Rolex Award instrument) uses stacked filters with a bandpass of 2.2 nm (FWHM). The second generation Microtops II (Solar Light Company instrument) uses filters with a bandpass of 2.5 nm (FWHM). These microprocessor-controlled TOPS have various combinations of from 3 to 5 UV-B filters. The best results have been had using filters with a peak transmission at 303 and 310 nm.

The calibration procedure has been described by Stanley Anderson in an unpublished report (Calibration procedure for Microtops, 1995) and by Morys, Mims and Anderson (1996). A paper describing the design and calibration of the first generation MicroTOPS is in preparation.

A comparison of ozone measurements by an EPA Brewer (no. 112), TOVS, SuperTOPS and MicroTOPS-7 from 8 Jun 1995 to 8 August 1995 yielded the results in Table A-1.

| Instrument | Total Ozone[1] | Std[1] | % Difference[2] | r |
|---|---|---|---|---|
| Brewer 112 | 291.2 | 6.5 | --- | --- |
| TOVS[3] | 285.7 | 6.1 | -1.9% | 0.42 |
| SuperTOPS | 293.9 | 6.6 | 0.9% | 0.69 |
| MicroTOPS-7 | 293.9 | 19.47 | 0.9% | 0.14 |

Notes:
1. Ozone is in Dobson units.
2. % compared instrument ozone is above or below Brewer ozone using -((Brewer/Ins)100)-100)
3. TOVS ozone data courtesy of Arthur Neuendorffer (NOAA NESDIS)

Table A-1. Comparison of mean total ozone near local solar noon measured by an EPA Brewer Spectrophotometer with ozone measured by TOVS, SuperTOPS and MicroTOPS-7 at Seguin, Texas, USA, from 8 Jun to 8 Aug 1995.

Table A-1 shows excellent agreement between the mean ozone measured over the 62-day comparision by the Brewer and both SuperTOPS and MicroTOPS-7. However, the standard deviation of measurements made with MicroTOPS-7 is 3 times greater than that of measurements made with SuperTOPS. This scatter is clearly reflected in the much lower correlation (r) of the latter with the Brewer. The scatter in the MicroTOPS-7 data is related to the haze which was present during the comparison.

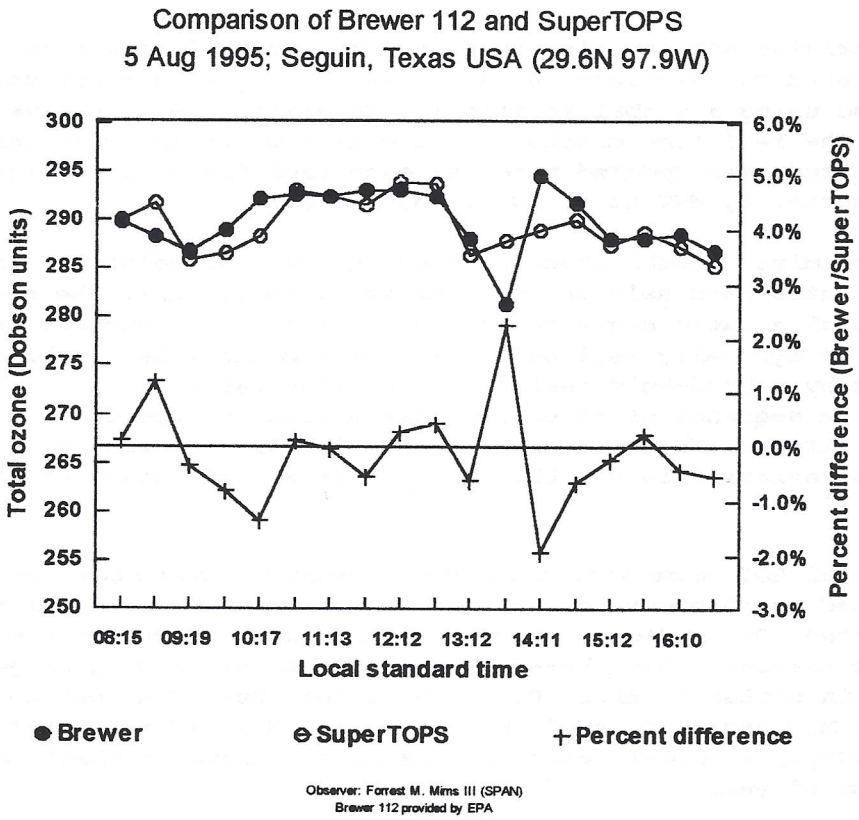


Fig. A-3. Comparison of total ozone measured by SuperTOPS and EPA Brewer Spectrophotometer 112 at Seguin, Texas USA on 5 August 1995.

Figure A-3 establishes that SuperTOPS lacks significant air mass dependence over the range of measurement times. The sharp dip in ozone measured by the Brewer at 1341 hrs occurred during passage of a small cumulus cloud past the solar disk. This event illustrates the advantage of a manually-operated instrument in such situtations since the SuperTOPS observation was intentionally delayed until just after the cloud moved away from the Sun.

## Appendix 5. Measurement Errors

The Sun photometers used in this study have a field of view of about 2 degrees. Since the Sun subtends 0.5 degree, increased circumsolar radiation caused by increased aerosols may cause a slight underestimate in the AOT. Volz (1974) measured underestimates of 0.003 and 0.008, respectively, at 500 nm for a hazy sky and a thin cirrus veil. Very slight errors may also be caused by temperature changes of the detectors, although this effect is minimized by keeping the instruments at or near room temperature until they are used.

Errors in deriving AOT can also be caused by errors in the time and coordinates used to calculate the air mass. During this study coordinates were measured using a Global Positioning Satellite (GPS) receiver (Magellan). The real time clocks of all data loggers and computers used during this study was updated prior to each each field trip using time signals broadcast by WWV at 5, 10, 15 and 20 MHZ.

Many tests by Mims (unpublished) have shown that the pointing error of a carefully pointed hand-held Sun photometer is negligible. The coefficient of variation of a rapid sequence of 5 or 10 scans, the numbers used during this study, is typically well below 1%. The excellent repeatability of measurements by a hand-held instrument is illustrated in Fig. A-4, a histogram of a sequence of 95 ozone observations by SuperTOPS, a MicroTOPS with 2.2 nm filters. The mean ozone amount is 259.3 Dobson units (DU), and the standard deviation is 0.8 DU, which gives a coefficient of variation of only 0.3%.

Measurements of $AOT_{\lambda}$ made with instruments used in this study were compared with published measurements of $AOT_{\lambda}$ for clear conditions. For example, Shaw (1982) measured $AOT_{\lambda}$ at Mauna Loa Observatory (MLO) at various wavelengths for all four seasons. Shaw showed that the clear-sky $AOT_{400nm}$ ranged from about 0.028 in winter to about 0.045 in spring. During a test on a very clear day at MLO near noon on 16 May 1996, the SUNTOPS used in this study yielded an $AOT_{376nm}$ of 0.037, which is reasonably close to Shaw's measurement for this time of year.

Confidence in the $AOT_{376nm}$ measurements in this study is also provided by measurements at 373.3 nm by a Reagan Sun photometer at the University of Arizona. Examples of unusually low $AOT_{373.3nm}$ measured by this instrument include 0.024 (27 Jun 1985), 0.023 (11 Jan 1986), 0.024 (2 Jan 1986) and 0.027 (26 Jan 1987). (These data were provided by John Simpson of the Institute of Atmospheric Physics at the University of Arizona.)

Confidence in the AOT measurements through severe aerosol loading in Alta Floresta is provided by the comparison of SUNTOPS observations in 1997 with Cimel measurements from Alta Floresta during SCAR-B in 1995 (see Fig. 4).

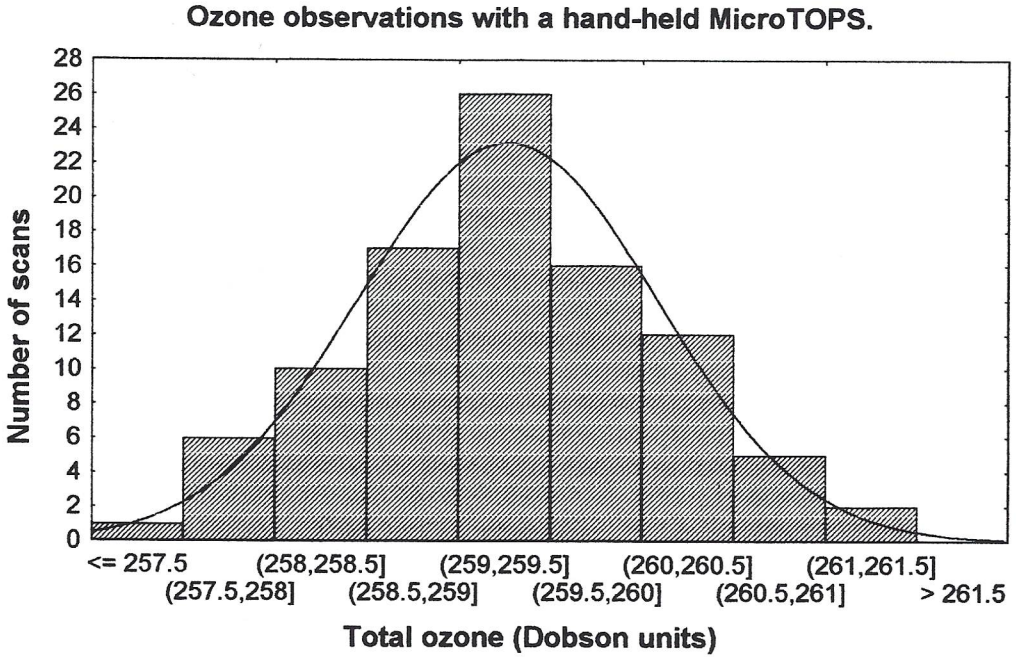


**Fig. A-4. Histogram of a sequence of 95 ozone observations by a hand held ozonometer.**

**Measurements of erythemally-weighted UV-B for this study were made using a Solar Light PMA radiometer, a Solar Light Probe and a custom made UV-B probe (response centered at 308 nm). These instruments all give results well correlated with observations by Brewer 112 and will be discussed in a paper in preparation (Mims, Rives and Barnard).**

**Errors in the measurement of total ozone are discussed in Appendix 4.**